

2012

## Hydrogen/Deuterium Exchange Studies of Protein and Non-Protein Amino Acids using Electrospray Ionization Mass Spectrometry

Justine Victoria Arrington  
*College of William & Mary - Arts & Sciences*

Follow this and additional works at: <https://scholarworks.wm.edu/etd>



Part of the [Biochemistry Commons](#)

---

### Recommended Citation

Arrington, Justine Victoria, "Hydrogen/Deuterium Exchange Studies of Protein and Non-Protein Amino Acids using Electrospray Ionization Mass Spectrometry" (2012). *Dissertations, Theses, and Masters Projects*. Paper 1539626931.

<https://dx.doi.org/doi:10.21220/s2-xnrb-dh49>

This Thesis is brought to you for free and open access by the Theses, Dissertations, & Master Projects at W&M ScholarWorks. It has been accepted for inclusion in Dissertations, Theses, and Masters Projects by an authorized administrator of W&M ScholarWorks. For more information, please contact [scholarworks@wm.edu](mailto:scholarworks@wm.edu).

Hydrogen/Deuterium Exchange Studies of Protein and Non-Protein Amino  
Acids Using Electrospray Ionization Mass Spectrometry

Justine Victoria Arrington

Rustburg, VA

Bachelor of Science, The College of William and Mary, 2010

A Thesis presented to the Graduate Faculty  
of the College of William and Mary in Candidacy for the Degree of  
Master of Science

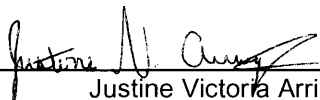
Department of Chemistry

The College of William and Mary  
January, 2012

## APPROVAL PAGE

This Thesis is submitted in partial fulfillment of  
the requirements for the degree of

Master of Science



---

Justine Victoria Arrington

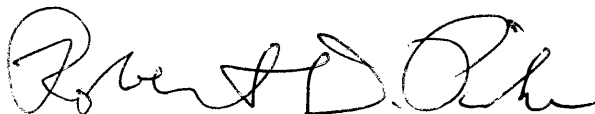
Approved by the Committee, August, 2011



---

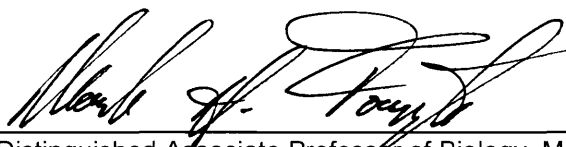
Committee Chair

Professor of Chemistry, John Poutsma  
The College of William and Mary



---

Garrett-Robb-Guy Professor of Chemistry, Robert Pike  
The College of William and Mary



---

Dorman Family Distinguished Associate Professor of Biology, Mark Forsyth  
The College of William and Mary

## ABSTRACT PAGE

In the studies detailed here, the hydrogen/deuterium exchange behavior of protonated lysine and its three homologs ornithine, 2,4-diaminobutyric acid (DABA), and 2,3-diaminopropionic acid (DAPA) was analyzed using an electrospray ionization ion trap mass spectrometer. Relative rate coefficients for the exchanges were calculated using a method to account for back exchange. Absolute rate coefficients were calculated using these relative rate coefficients and the concentration of D<sub>2</sub>O in the ion trap, as determined by analysis of the single exchange of betaine. The four amino acids were observed to exchange all six of their labile hydrogens. The exchange rate coefficients for ornithine were slower than those of lysine, DABA, and DAPA by at least a factor of 15. Optimized structures for protonated lysine, ornithine, DABA, and DAPA were obtained at the B3LYP/6-31+G\*\* level of theory. The interactions of water with protonated ornithine, DABA, and DAPA were also modeled at the same level. It was discovered that the energetic barriers to exchange for ornithine and DAPA via the flip-flop and relay mechanisms differed by only 0.8 kcal/mol and 1.9 kcal/mol, respectively.

In a second set of studies, the H/D exchange behavior of protonated arginine and its oxa-analog canavanine was analyzed using the aforementioned mass spectrometer. Protonated monomeric arginine did not undergo significant exchange under the experimental conditions, whereas protonated monomeric canavanine was observed to exchange all eight of its labile hydrogens. The proton-bound arginine dimer, however, exchanged all 15 of its labile hydrogens at a faster rate than the proton-bound canavanine dimer. It is proposed that a salt bridge complex in which one amino acid is a zwitterion and the other is in a charge solvated form would explain the H/D exchange behavior of the proton-bound arginine dimer.

## Table of Contents

|                       |     |
|-----------------------|-----|
| Acknowledgements..... | iii |
| List of Figures ..... | iv  |
| List of Tables .....  | v   |

### **Chapter 1: General Introduction to H/D Exchange Mass Spectrometry**

|  |   |
|--|---|
| 1.1 Studying Protein Conformations.....        | 1 |
| 1.2 H/D Exchange Studies in Solution .....     | 5 |
| 1.3 H/D Exchange Studies in the Gas Phase..... | 6 |
| 1.4 References.....                            | 8 |

### **Chapter 2: Experimental and Theoretical Procedures**

|                                   |    |
|-----------------------------------|----|
| 2.1 Experimental Procedures ..... | 10 |
| 2.2 Theoretical Procedures.....   | 18 |
| 2.3 References.....               | 19 |

### **Chapter 3: H/D Exchange Behavior of Lysine and its Homologs**

|                                   |    |
|-----------------------------------|----|
| 3.1 Introduction.....             | 20 |
| 3.2 Experimental Procedures ..... | 22 |
| 3.3 Results.....                  | 24 |
| 3.4 Discussion.....               | 31 |
| 3.5 References.....               | 36 |

### **Chapter 4: H/D Exchange Behavior of Arginine and Canavanine**

|                                   |    |
|-----------------------------------|----|
| 4.1 Introduction.....             | 38 |
| 4.2 Experimental Procedures ..... | 41 |
| 4.3 Results.....                  | 42 |

4.4 Discussion.....46

4.5 References.....47

**Chapter 5: Conclusions**

5.1 Study of Protonated Lysine and its Homologs .....49

5.2 Study of Protonated Arginine and Canavanine.....50

## **Acknowledgements**

First, I would like to thank my research advisor, Professor John Poutsma, for his guidance and support over the past two and a half years. I have learned a lot about the research process from him, and he has made me realize how much fun it can be to study chemistry. I also appreciate the family and friends who have encouraged me to do my best and see the humor in things (that includes everyone in Ionlab!). I could not have made it without them. Finally, I would like to thank Professor Robert Pike and Professor Mark Forsyth for serving on my committee and providing valuable feedback.

## List of Figures

|  |    |
|--|----|
| Figure 1.1 Proposed mechanisms of H/D exchange .....                                   | 7  |
| Figure 2.1 Schematic diagram of the ion trap mass spectrometer .....                   | 11 |
| Figure 2.2 Schematic diagram of the helium inlet system.....                           | 12 |
| Figure 3.1 Structures of lysine, lysine's homologs, and betaine .....                  | 21 |
| Figure 3.2 a,b Mass spectra for protonated lysine and ornithine .....                  | 27 |
| Figure 3.2 c,d Mass spectra for protonated DABA and DAPA.....                          | 28 |
| Figure 3.3 a,b Simple and <sup>13</sup> C fits done with KinFit .....                  | 29 |
| Figure 3.3 c Back exchange fit done with KinFit.....                                   | 30 |
| Figure 3.4 Lowest energy structures for protonated lysine and its homologs .....       | 33 |
| Figure 3.5 PES for the interaction of water with protonated DAPA .....                 | 35 |
| Figure 4.1 Conversion of a generic amino acid into its corresponding zwitterions ..... | 38 |
| Figure 4.2 Salt bridge structure of the proton-bound arginine dimer .....              | 40 |
| Figure 4.3 Comparison of the structures of arginine and canavanine.....                | 40 |
| Figure 4.4 Mass spectra for protonated canavanine and arginine.....                    | 43 |
| Figure 4.5 Mass spectra for the proton-bound dimers of canavanine and arginine.....    | 45 |



## List of Tables

|   |    |
|---|----|
| Table 3.1 Rate coefficients for the H/D exchange of lysine and its homologs.....                        | 30 |
| Table 3.2 Calculated barriers to H/D exchange mechanisms for protonated<br>lysine and its homologs..... | 34 |
| Table 4.1 Relative rate coefficients for the H/D exchange of two<br>proton-bound dimers.....            | 44 |

## Chapter 1: General Introduction to H/D Exchange Mass Spectrometry

### 1.1 Studying Protein Conformations: Physical Techniques and H/D Exchange

Hydrogen/deuterium (H/D) exchange, a type of reaction in which a labile hydrogen atom is replaced by a heavier isotope of hydrogen, has become an increasingly important tool for studying protein structure and dynamics. In the 1950s, Linderstrøm-Lang and co-workers recognized that the H/D exchange rates of backbone amides in proteins were affected by protein structure that was a result of hydrogen bonding.<sup>1</sup> It is generally understood that protein structure heavily influences protein function. Furthermore, proteins can undergo conformational changes as a result of ligand binding, modification, and interactions with other proteins. These conformational changes can then alter the ability of enzymes to catalyze other reactions.<sup>1</sup> Thus, characterizing changes in protein conformation can also give critical insight into enzyme functionality, and the fact that monitoring H/D exchange kinetics can provide just this sort of information has caused the popularity of the technique to skyrocket in recent years.

Observing protein conformation changes is possible with a variety of other techniques including fluorescence measurements, circular dichroism (CD) spectroscopy, nuclear magnetic resonance (NMR) spectroscopy, and mass spectrometry.<sup>2,3</sup> Fluorescence can be used to evaluate how many aromatic amino acids are in contact with the solvent surrounding the protein of interest; thus, fluorescence measurements can serve as “markers of dynamic events.”<sup>3</sup> CD spectroscopy in the ultraviolet region can be used to gauge variations in the secondary structure of proteins, but unlike NMR, it cannot provide information about the spatial relationships among specific portions of the protein.<sup>2</sup> Because NMR provides data at the residue level and can be used to study protein

dynamics over a wide range of time scales,<sup>3</sup> it has been widely utilized in studying conformational changes and has been the traditional choice for coupling with H/D exchange reactions. The combination of H/D exchange methods with mass spectrometry to analyze protein conformations is newer, having been pioneered during the early 1990s,<sup>4</sup> but mass spectrometry itself has several advantages over NMR. For instance, mass spectrometric analyses can be conducted with protein concentrations of less than a micromole, so a smaller amount of sample material is needed than with NMR.<sup>1,3</sup> In addition, while it can be challenging to use NMR to study proteins larger than approximately 50 kDa, there is “no practical size limitation” on the proteins that can be analyzed with mass spectrometry.<sup>1</sup>

In a 1990 communication, Chowdhury, Katta, and Chait reported using mass spectrometry to analyze protein conformational changes in three dimensions for the first time. The researchers employed a mass spectrometer equipped with an electrospray ionization (ESI) source,<sup>5</sup> which was a newly developed source at the time.<sup>4</sup> ESI is a “soft” ionization technique, meaning that as molecules are ionized and moved from solution into the gas phase for entry to the mass analyzer, they are less likely to fragment than with “hard” ionization techniques. Chowdhury, Katta, and Chait took advantage of ESI to create “intact multiply charged gas phase ions” from proteins in solution.<sup>5</sup> The ions were multiply charged because they were produced through the protonation of accessible basic sites on protein molecules. Therefore, an unfolded protein should have had a larger number of accessible basic sites and should also have had a higher charge state, as reflected by the mass spectrum, than a tightly folded protein. This assumes, of course, that the charge states of the proteins in the gas phase corresponded to the charge

states of the proteins in solution, where the conformational changes were induced. The researchers noted that at least three conformations of bovine cytochrome c had been described with other techniques under acidic pH. Interestingly, Chowdhury, Katta, and Chait also found bovine cytochrome c to have three separate charge states in the gas phase—and thus three separate conformations—as they varied the pH of their sample solutions from 2.6 to 5.2.<sup>5</sup>

Less than a year later, Katta and Chait published another communication in which they described coupling H/D exchange reactions to the previously described method of probing protein conformational changes with the charge states produced by ESI mass spectrometry.<sup>2</sup> The researchers observed that, as with the distribution of charge states, the levels of H/D exchange for a given protein should vary with conformation. In other words, large amounts of exchange are expected for a denatured protein in which most of the labile hydrogens were exposed to a deuterated solvent. Tightly folded proteins, however, should undergo lower levels of exchange in the same amount of time because some of their labile hydrogens are located within the hydrophobic center of the protein or are involved in hydrogen bonds.<sup>2</sup> Katta and Chait examined bovine ubiquitin under two sets of conditions. First, the protein was dissolved in D<sub>2</sub>O with 1% deuterated acetic acid for 20 minutes before being analyzed with mass spectrometry. Then, a new sample of the protein was dissolved in a mixture of deuterated acetic acid, D<sub>2</sub>O, and deuterated methanol in a 1:99:100 ratio by volume for 23 minutes before being analyzed with mass spectrometry. The researchers found that the first sample of ubiquitin had two dominant charge states: the 8+ and 7+ charge states. This was in agreement with the previously characterized crystal structure of ubiquitin, which indicated only seven or eight basic

sites would be available for protonation in the protein's native conformation. They also found that only 62% of ubiquitin's 144 labile hydrogens had been exchanged for deuterium atoms under the first set of conditions.<sup>2</sup> Under the second set of conditions, the researchers found a larger charge distribution for ubiquitin, with the 10+ charge state being the dominant peak in the spectra. Therefore, the addition of methanol had resulted in at least partial unfolding of the protein and had made more sites accessible for protonation. Moreover, although the protein molecules were exposed to deuterium atoms for similar time periods in both cases, the spectra obtained under the second set of conditions indicated that 91% of the labile hydrogens in ubiquitin had undergone exchange.<sup>2</sup>

The studies done by Chowdhury, Katta, and Chait show that mass spectrometry is a valid technique for studying protein conformational changes. More importantly though, their research highlights why mass spectrometry is an excellent choice for coupling with H/D exchange reactions. Mass spectrometry can easily be used to monitor H/D exchange reactions because each exchange results in a change in mass for the molecule of interest, which is indicated directly on the mass spectrum. Mass spectrometry also provides users with the advantage of being able to detect and characterize protein conformations that exist in solution at the same time at equilibrium.<sup>3</sup> Thus, over the two decades since the publication of the previously described communications, much research has been done to expand upon this combination of techniques and utilize it to its fullest potential. In the following sections of this chapter, some of the types of experiments that can be done with mass spectrometry and H/D exchange will be outlined along with the challenges in implementing or interpreting the results of such experiments. This discussion will

elucidate the reasons for undertaking the current studies, which are detailed at length in later chapters.

## 1.2 H/D Exchange Studies in Solution

There are a variety of H/D exchange mass spectrometry experiments that can be performed with proteins that have been exposed to a deuterating agent in solution. However, the majority of these experiments are similar in that their focus is on the exchange of the backbone amide hydrogens. These exchanges may happen within a matter of seconds or may take several months.<sup>4</sup> In general, the backbone amide hydrogens of an unfolded protein will exchange more quickly than those of the same protein in a tightly folded conformation. Backbone amide hydrogens in folded proteins tend to be involved in hydrogen bonds, which limit the rate at which exchange can occur. Other backbone amide hydrogens may be buried within a folded protein, which limits solvent interactions and reduces rates of H/D exchange.<sup>6</sup>

Solution phase H/D exchange of proteins can be accomplished in a couple of ways. In the first experimental setup, folding changes are induced by exposing the proteins to denaturing agents, pH changes, or temperature changes. Then, the proteins are exposed to a pulse of D<sub>2</sub>O for a very short amount of time before the reaction is quenched. The proteins that are unfolded will be isotopically labeled with deuterium atoms while the proteins that are folded will remain unlabeled. Upon analysis with mass spectrometry, researchers will gain information about the populations of folded and unfolded proteins at a particular time.<sup>4</sup> In the second major experimental setup, proteins are dissolved in D<sub>2</sub>O while they are undergoing folding changes. Multiple samples are

removed over time for quenching and analysis. This type of experiment can provide information about conformational intermediates.<sup>4</sup>

Once labeled, the proteins can be analyzed via mass spectrometry to determine how many hydrogen atoms were replaced; this is called a global exchange analysis because it provides levels of deuterium incorporation for whole proteins.<sup>4</sup> On the other hand, if the biological function of a protein is being analyzed, “the actual number of deuterons that have exchanged is not as important as where the exchange has occurred.”<sup>4</sup> In this case, it would be more appropriate to digest the labeled protein and study its fragments. This type of local exchange analysis provides a measure of spatial resolution when studying deuterium incorporation. However, digestion of larger proteins tends to produce longer peptides, which can make data interpretation more difficult. Furthermore, there are few acid proteases suited for the digestion step, and the most efficient acid protease is non-specific.<sup>4</sup>

### 1.3 H/D Exchange Studies in the Gas Phase

Although it may initially seem counterintuitive, studying protein conformational changes with H/D exchange in the gas phase can provide useful information about protein conformations in the solution phase. Green and Lebrilla note that there are no set rules regarding the extent to which gas phase and solution phase conformations will correspond to one another. Considering the effects that hydrophobicity and hydrogen bonding have on protein conformations, one can almost expect certain differences to exist between gas and solution phase.<sup>6</sup> However, many groups—including Green and Lebrilla—have also observed that comparing gas phase and solution phase conformational changes provides insights on the degree to which solvent interactions

affect protein folding.<sup>6-8</sup> Additionally, because gas phase conformations of proteins do not seem to interconvert unless there is a perturbing agent present, gas phase H/D exchange studies may make it possible to analyze folding intermediates that exist in solution for only a short time.<sup>6,8</sup>

Analysis of proteins and other biomolecules with H/D exchange mass spectrometry in the gas phase can be made more complicated by the influences of amino acid side chains. The exchange rates and mechanisms of amino acids in solution are well documented, but this work in the gas phase is still ongoing.<sup>9</sup> Campbell and co-workers studied the H/D exchange of glycine oligomers in the gas phase with a Fourier-transform ion cyclotron resonance mass spectrometer and proposed several mechanisms (see Figure

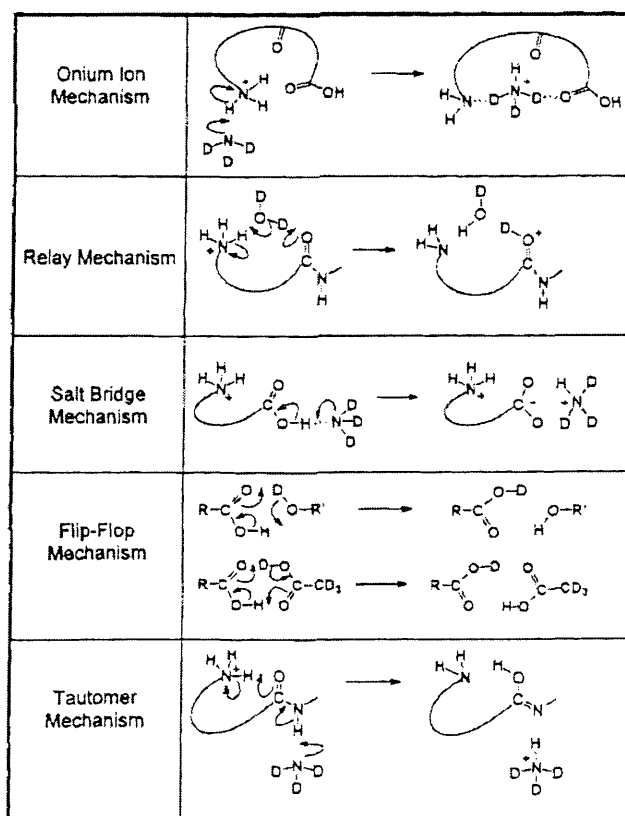


Figure 1.1 Proposed mechanisms of H/D exchange for glycine oligomers. Taken from Campbell and co-workers<sup>10</sup>



1.1 for a summary of the mechanisms) based on experimental results and semiempirical calculations.<sup>10</sup> Because the current studies involving the H/D exchange behavior of protonated amino acids use D<sub>2</sub>O as the deuterating reagent, the relay and flip-flop mechanisms are most relevant ones to discuss here. In the relay mechanism, the D<sub>2</sub>O molecule essentially shuttles a proton from the protonated N-terminus to another site on the amino acid; this second site is usually, but not necessarily always, the amide oxygen.<sup>10</sup> The flip-flop mechanism, however, is multi-centered and accounts for the exchange of the labile hydrogen at the C-terminus when a less basic deuterating reagent is employed. These mechanisms seem straightforward, but Campbell and co-workers caution that the incorporation of other more basic amino acids such as arginine could complicate the exchange process.<sup>10</sup>

#### 1.4 References

1. Busenlehner, L. S.; Armstrong, R. N. *Archives of Biochemistry and Biophysics* **2005**, *433*, 34-46.
2. Katta, V.; Chait, B. T. *Rapid Commun. Mass Spectrom.* **1991**, *5*, 214-217.
3. Kaltashov, I. A.; Eyles, S. J. *J. Mass Spectrom.* **2002**, *37*, 557-565.
4. Wales, T. E.; Engen, J. R. *Mass Spectrom. Rev.* **2006**, *25*, 158-170.
5. Chowdhury, S. K.; Katta, V.; Chait, B. T. *J. Am. Chem. Soc.* **1990**, *112*, 9012-9013.
6. Green, M. K.; Lebrilla, C. B. *Mass Spectrom. Rev.* **1997**, *16*, 53-71.
7. Evans, S. R.; Lueck, N.; Marzluff, E. M. *Int. J. Mass Spectrom.* **2003**, *222*, 175-187.
8. Wood, T. D.; Chorush, R. A.; Wampler, F. M., III; Little, D. P.; O'Connor, P. B.; McLafferty, F. W. *Proc. Natl. Acad. Sci. USA* **1995**, *92*, 2451-2454.
9. Evans, S. E.; Lueck, N.; Marzluff, E. M. *Int. J. Mass Spectrom.* **2003**, *222*, 175-187.

10. Campbell, S.; Rodgers, M. T.; Marzluff, E. M. Beauchamp, J. L. *J. Am. Chem. Soc.* **1995**, *117*, 12840-12854.

## Chapter 2: Experimental and Theoretical Procedures

### 2.1 Experimental Procedures

All experimental work was done using a modified Thermo-Finishing LCQ DECA quadrupole ion trap mass spectrometer equipped with an external electrospray ionization (ESI) source; see Figure 2.1 below for a general diagram of the instrument. A KD Scientific syringe pump with a 500  $\mu$ L Hamilton gas-tight syringe (model #1750, cemented needle) was used to introduce sample solutions to the ESI source through fused silica capillaries. In the experiments detailed here, the sample solutions always contained acetic acid, which served as a proton source for the sample. Thus, the sample solution droplets entering the source were positively charged. A positive voltage on the ESI needle propelled the positively charged droplets toward the heated capillary. As the droplets moved through the heated capillary, the solvent evaporated, decreasing the surface area to charge ratio of the droplets. Through a series of Coulombic explosions due to the buildup of charge, the droplets were ripped apart into smaller and smaller micro-droplets. Finally, the solvent was completely evaporated, leaving behind pseudo-molecular ions in the gas phase that could enter the trap for analysis. The Xcalibur software suite (version 1.3) installed on the Dell desktop computer running Windows 2000 Professional attached to the mass spectrometer was used to control instrument operations, display the mass spectrum corresponding to the contents of the ion trap, and collect data.

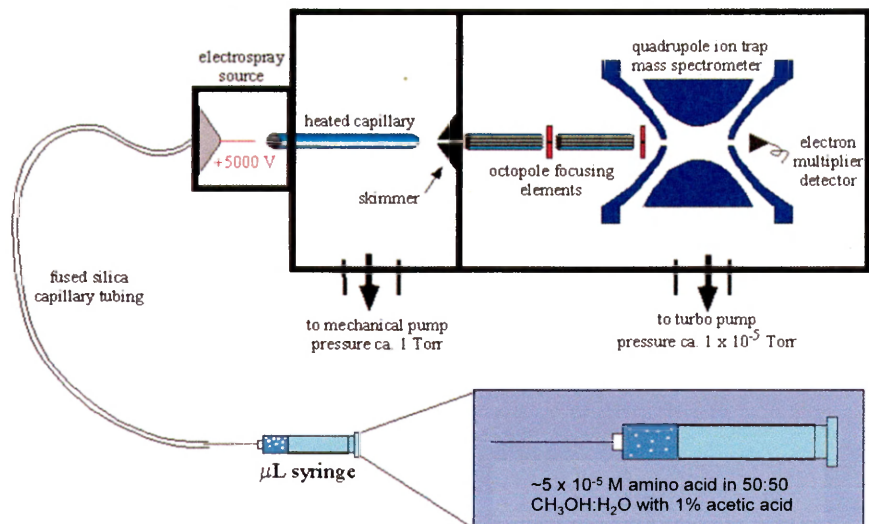


Figure 2.1 Schematic diagram of the ion trap mass spectrometer

The LCQ DECA mass spectrometer was modified for these experiments during the summer of 2009 (see Figure 2.2 for a diagram of the modifications). More specifically, the original helium inlet that entered the left side of the instrument was disconnected at the ion trap. A new helium inlet was then run to the trap through an opening cut into the top of the mass spectrometer. The new inlet system consisted of a helium tank that was connected to a purifier (VICI Metronics) to remove impurities such as hydrocarbons, moisture, and oxygen. This filter was then connected to a flow-meter which was responsible maintaining a constant helium flow. The gas line exiting the flow-meter ran to a T-joint that could be capped as needed; another gas line ran from the opposite side of the T-joint to an SGE Incorporated micro needle valve (MCVT-1 1/50). The capped side of the T-joint could be uncapped and connected to 1/8" diameter PEEK tubing; this tubing was connected to a second Hamilton 500  $\mu\text{L}$  gas-tight syringe. Combined with a Fisher Scientific syringe pump to control the flow rate, the second

syringe was used to introduce neutral reagents such as liquid D<sub>2</sub>O to the helium inlet system. Provided that the flow rate of the neutral reagent was low (400 μL/hour or lower), the incoming helium could transport the reagent in the gas phase. Excess helium and reagent gas was allowed to exit one side of the micro needle valve while the remaining gas was directed to the trap through 1/16" diameter stainless steel tubing.

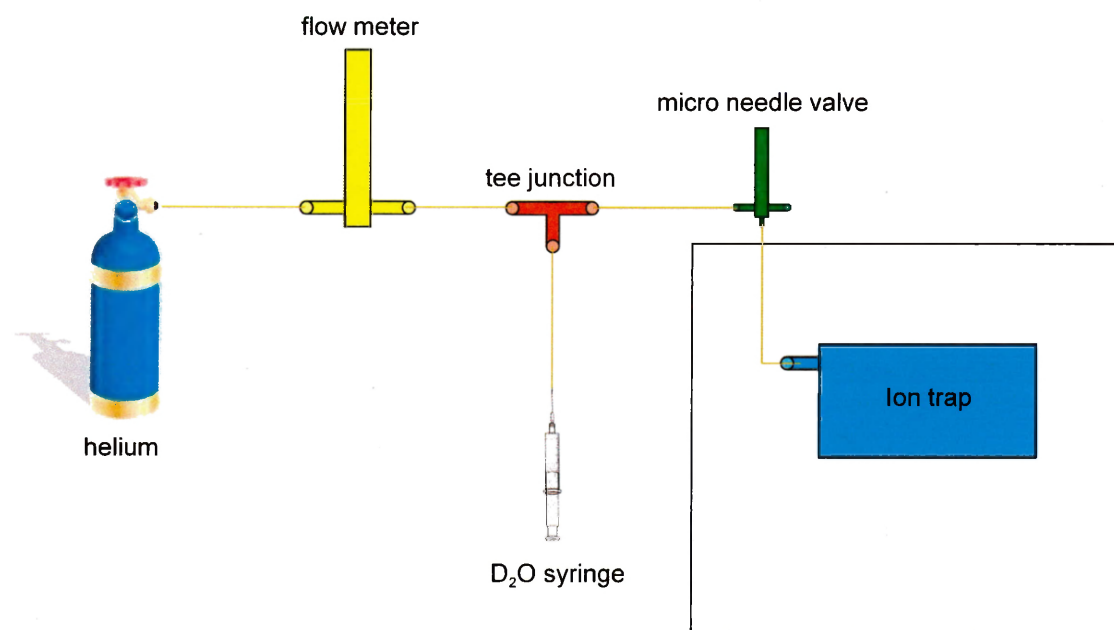


Figure 2.2 Schematic diagram of the helium inlet system

Between experiments, the ESI source of the ion trap mass spectrometer was opened, and a septum was placed over the heated capillary to allow the instrument to maintain a vacuum of  $0.1$  to  $0.3 \times 10^{-5}$  Torr at the ionization gauge. At the beginning of an experiment, the septum was removed, and the ESI source was closed by tightening two thumbscrews on the front of the source. Then, the helium tank and helium regulator were opened; to conserve helium, these were closed at the end of each experiment.

Nitrogen served as a sheath gas to direct the droplets formed by the ESI source through the heated capillary, but since a very low flow rate of the gas was needed for this function, the nitrogen tank and nitrogen regulator could be left open at all times without fear of wasting large amounts of nitrogen. After opening the helium tank, the LCQ Tune program of the Xcalibur software suite was used to bring the instrument out of standby mode. LCQ Tune also displayed an instrument status panel on the right side of the computer monitor. While watching the ion gauge pressure reading in the instrument status panel, the micro needle valve was opened, causing the ion gauge pressure to increase. Experiments were typically conducted at an ion gauge pressure of 1.3 to 2.2 x 10<sup>-5</sup> Torr. Next, LCQ Tune was used to adjust the temperature of the heated capillary to 120 to 125°C. While the heated capillary temperature and ion gauge pressure were settling to constant readings, a flush of 50:50 methanol and water was introduced to the ESI source; the HPLC grade methanol was obtained from Fisher Scientific, and the water had been purified via a Millipore system. As its name implies, this flushing mixture was used to clear the trap of ions from previous experiments. For H/D exchange experiments, the T-joint of the helium inlet system was uncapped, and a syringe of D<sub>2</sub>O was started while the pressure and temperature readings were becoming steady. The purpose of starting the flow of D<sub>2</sub>O before introducing an actual sample was to “season” the trap. By replacing as much water on the surface of the trap as possible with D<sub>2</sub>O, it could be assumed that D<sub>2</sub>O was abundant in the trap. Thus, the H/D exchange reactions of the samples could be treated as pseudo-first-order reactions, and back exchange of deuterium atoms for hydrogen atoms via a reaction with H<sub>2</sub>O would be limited.

Once the temperature and pressure readings were constant, the syringe of flush was removed from the KD Scientific syringe pump. The syringe was cleaned with methanol and filled with a sample solution; then, the syringe was replaced on the pump, the pump was reset with the correct solution volume, and the pump was turned on. After a few minutes, the presence of a peak on the mass spectrum displayed by LCQ Tune corresponding to the mass to charge ratio of the protonated parent ion indicated that the sample had reached the trap. Next, the auto-tune function of LCQ Tune was used to adjust various settings to optimize the detection of the  $m/z$  ratio of interest. Then, the protonated parent peak was isolated using tandem mass spectrometry (MS/MS mode), and the parent peak with its corresponding exchange peaks was further resolved in zoom scan mode. Data collection of at least 10 scans per activation time was completed through LCQ Tune. Data was collected at multiple activation times (from 1 ms to 15 s) so all of the possible exchanges could be observed since longer activation times corresponded to longer reaction times between the  $D_2O$  molecules and the sample ions in the trap. To account for systematic errors caused by drifting pressure, half of the spectra were collected in order of increasing activation time. Then, the remaining half were recorded in order of decreasing activation time with each new activation time falling between two activation times previously collected. These spectra were saved on the computer attached to the mass spectrometer under the appropriately named folder with the date the data was collected. Once the necessary spectra were saved, the sample syringe was cleaned with methanol and filled with the flushing mixture. At least 500  $\mu\text{L}$  of flushing solution was directly infused into the source before another sample solution was analyzed; this ensured that the ion count of the current sample was high and that the current sample was not

competing with a previous sample for D<sub>2</sub>O. It is also important to note that the D<sub>2</sub>O syringe pump ran continuously throughout the experiment so the assumption of pseudo-first-order rate kinetics remained valid.

After spectra were collected for all of the samples following the procedure outlined above (sample introduction in MS mode, auto-tuning on the peak of interest, isolation in MS/MS mode, and data collection in zoom scan mode at various activation times) the instrument was flushed again. Then, the needle valve, helium regulator, and helium tank were closed. LCQ Tune was used to lower the heated capillary temperature to 80°C and to put the instrument in standby mode. Finally, the thumb screws on the ESI source were loosened, and the septum was replaced over the heated capillary. The H/D exchange data was then analyzed using the QualBrowser portion of Xcalibur, Microsoft Excel 2002, and the KinFit kinetics fitting routine of Nicoll and Dearden<sup>1</sup> on a second Dell desktop computer running Windows XP Professional in the laboratory.

First, the data files with the .RAW extension were opened with QualBrowser, which displays a graph of relative ion abundance versus time at the top of the window and an actual mass spectrum at the bottom of the window. To consider all of the scans taken at a particular activation time, the mouse was used to drag a single line across the entire top graph; this instructed QualBrowser to display the average of the total spectra collected in the bottom panel. This step was only modified when there was a clear decrease in ion counts as shown in the top graph. For instance, if it was noted that the sample syringe pump stopped midway through a scan and this was reflected in the ion abundance graph, then a line was dragged from the beginning of collection to the point at which the signal dropped and presumably the point at which the syringe pump stopped.



Next, an additional menu was displayed by right clicking on the averaged mass spectrum. The options “Export” and “Clipboard (Nominal Mass)” were chosen to copy the data over to the clipboard that was accessible to Microsoft Office programs.

After copying data to the clipboard, Microsoft Excel was opened, and the data was pasted into the first worksheet in the form of a table of nominal mass versus relative intensity. Then, the .RAW file of the next longer activation time was opened with QualBrowser; the process explained above was used to copy the data from this file into a different portion of the Excel worksheet. This was continued until all of the nominal mass data had been copied into Excel. Next, the second worksheet of the workbook was opened. A table of time in seconds versus the intensity of various exchange peaks was constructed. For the sake of simplicity, the column listing the intensity data for the parent peak was labeled D0, the column listing the intensities of the first exchange peak over time was labeled D1, and so on; the D stood for deuterium, and the number following indicated the number of deuterium atoms that had been incorporated in place of hydrogens. Once the labels for this table were in place, intensity data was copied from the first worksheet into the appropriate cells of the table. For example, if it was known that the parent ion had a mass of 150 and that six exchange peaks were expected, ion intensities from a mass of 150 to a mass of 156 at that activation time were copied; the data was then pasted into the appropriate row of the table on the second worksheet via the “Paste Special” and “Transpose” commands of Excel. This process was repeated until all of the necessary intensity data at the various activation times had been copied into the table. Then, a “Total” column was labeled to the right of the table. At each activation time, the intensities for all of the exchange peaks were summed in the corresponding cell

of the Total column. Finally, the labels from the table were copied into a different set of cells on the second worksheet. The data from the first table was normalized in the second table by dividing each intensity by the appropriate cell of the Total column from the first table. This procedure helped account for small changes in signal over time by making it possible to examine the ratios of the parent and exchange peaks instead of the actual ion counts.

The final step in analyzing the data involved the KinFit fitting routine, which was made into an add-on for Excel that could be used to solve coupled differential equations. The KinFit menu could be accessed by first loading it as an add-on under the “Tools” menu of Excel. Once the KinFit menu was visible, the option “Change ODEs” was selected. This command opened a separate Excel workbook associated with the add-on that had a variety of previously saved differential equations. From this point, it was possible to either copy the equations from the associated workbook or to simply type them out. In the first workbook containing the data for analysis, the Tools menu was opened. From this menu, the “Macro” menu was opened, and “Visual Basic Editor” was selected. This opened the Visual Basic scripts associated with the KinFit add-on and made it possible to input which differential equations should be used for a given data set. These equations changed according to the level of analysis complexity as well as the number of expected exchanges; the different analysis methods and the needed equations will be described in further detail in a later chapter. For now, it is necessary to simply note that the equations could be changed. Once the equations had been entered, the “File” menu of the Visual Basic Editor was opened, and the “Close and Return to Excel” option was selected. From the first workbook, the KinFit menu was opened, and the “ODE

Change Finish” option was selected. Then, the “Fit Data” command from the KinFit menu was selected. The normalized data was selected, and after inputting the number of expected rate constants as well as a name for a new worksheet, KinFit attempted to iteratively solve the differential equations. KinFit then generated a new worksheet listing the rate constants that provided the best fit with the given set of equations. This new worksheet also contained the option to “Make a Graph” so it was possible to see how well the equations with the newly solved rate constants fit the data. Here, it is important to point out that this process only works with older versions of Microsoft Excel because the ability to use the Visual Basic Editor was disabled in later editions; thus, it is difficult if not impossible to change the differential equations that the KinFit add-on uses in versions of Excel that came out after 2003.

## 2.2 Theoretical Procedures

To guide further experimentation and to help explain the results of previously completed experiments, theoretical calculations were performed with GaussView 2.1 and Gaussian 98W<sup>2</sup> on one Dell desktop running Windows XP Professional and four computers running Linux 2.4.21 (Red Hat Enterprise Linux version 3). Files were transferred among these computers using the F-Secure SSH File Transfer Client (version 5.2), and commands to run or modify input files with Gaussian 98W on the four Linux computers were executed via the F-Secure SSH Client (version 5.2) running on the Dell desktop. In general, the structures of the compounds of interest were drawn in GaussView and submitted to Gaussian 98W for geometry optimization at the Hartree-Fock level of theory with the 3-21G basis set. Transition states were located using the Hartree-Fock method and the 3-21G basis set with the Opt(TS) keyword; the keywords

Opt(TS, CalcFC) and Opt(TS, CalcAll) were also used when initial attempts at finding a transition state were unsuccessful. Once chemically reasonable structures had been obtained, the structures were re-optimized with density functional calculations at the B3LYP level of theory with the 6-31+G\*\* basis set. The suspected transition structures were further characterized by calculating their vibrational frequencies with the Opt(Freq) keyword at the B3LYP level of theory with the 6-31+G\*\* basis set. The presence of only one negative eigenvalue in the Hessian matrix (represented as a negative frequency in GaussView) was used as confirmation that the structure in question was indeed a transition state.

### 2.3 References

1. Nicoll, J. B.; Dearden, D. V. *KinFit: Kinetics Fitting for Coupled Ordinary Differential Equations*, version 2.0; Department of Chemistry and Biochemistry, Brigham Young University: Provo, UT, 2003.
2. *Gaussian 98*, Revision A.9; Frisch, M. J.; Trucks, G. W.; Schlegel, H. B.; Scuseria, G. E.; Robb, M. A.; Cheeseman, J. R.; Zakrzewski, V. G.; Montgomery, J. A., Jr.; Stratmann, R. E.; Burant, J. C.; Dapprich, S.; Millam, J. M.; Daniels, A. D.; Kudin, K. N.; Strain, M. C.; Farkas, O.; Tomasi, J.; Barone, V.; Cossi, M.; Cammi, R.; Mennucci, B.; Pomelli, C.; Adamo, C.; Clifford, S.; Ochterski, J.; Petersson, G. A.; Ayala, P. Y.; Cui, Q.; Morokuma, K.; Malick, D. K.; Rabuck, A. D.; Raghavachari, K.; Foresman, J. B.; Cioslowski, J.; Ortiz, J. V.; Baboul, A. G.; Stefanov, B. B.; Liu, G.; Liashenko, A.; Piskorz, P.; Komaromi, I.; Gomperts, R.; Martin, R. L.; Fox, D. J.; Keith, T.; Al-Laham, M. A.; Peng, C. Y.; Nanayakkara, A.; Challacombe, M.; Gill, P. M. W.; Johnson, B.; Chen, W.; Wong, M. W.; Andres, J. L.; Gonzalez, C.; Head-Gordon, M.; Replogle, E. S.; Pople, J. A. Gaussian, Inc.: Pittsburgh, PA, 1998.

## Chapter 3: H/D Exchange Behavior of Lysine and its Homologs

### 3.1 Introduction

H/D exchange reactions are used as probes of biomolecule structure and show great promise for elucidating protein conformational changes when combined with mass spectrometry. However, given the variety of proposed mechanisms by which these reactions can occur, it is clear that the process of H/D exchange is not fully understood. Many attempts have been made to investigate the H/D exchange behavior of compounds with only one type of functional group.<sup>1</sup> For instance, Ausloos and Lias studied H/D exchange reactions of protonated monofunctional compounds in the gas phase with a pulsed ion cyclotron resonance mass spectrometer. The monofunctional compounds studied included alcohols, acids, mercaptans, H<sub>2</sub>S, AsH<sub>3</sub>, PH<sub>3</sub>, and aromatic molecules.<sup>2</sup> The efficiency of H/D exchange reactions is thought to be affected by the endothermicity or exothermicity of the proton (deuteron) transfer from the deuterated reagent to the second molecule. Specifically, Ausloos and Lias found that H/D exchange was not observed when the proton transfer reaction was more than approximately 20 kcal/mol endothermic.<sup>2</sup> In other words, H/D exchange reactions did not occur between molecules with proton affinity (PA) differences of more than 20 kcal/mol,<sup>3</sup> where proton affinity is defined as the negative of the enthalpy for a protonation reaction. However, when studying H/D exchange reactions between ND<sub>3</sub> and protonated peptides with a four sector tandem mass spectrometer, Cheng and Fenselau found that H/D exchange occurred even when the PA of the peptide exceeded that of the deuterated base by more than 50 kcal/mol.<sup>4</sup> Therefore, there are interesting differences between the H/D exchange

reactions of compounds with one functional group and compounds with multiple functional groups.

If the overarching goal is to better understand H/D exchange as it pertains to biomolecules, then it is necessary to further investigate H/D exchange reactions with polyfunctional compounds. It is also important, however, to consider the simplicity of the polyfunctional compound. For instance, Gard and co-workers caution that peptides and proteins may be too complex for studying the relationship between the site of protonation and the site of H/D exchange.<sup>1</sup> Amino acids, on the other hand, make ideal candidates for study with H/D exchange because they are simpler than peptides and proteins and are readily available. In the current study, the H/D exchange behavior of the protonated amino acids lysine, ornithine, 2,4-diaminobutyric acid (DABA), and 2,3-diaminopropionic acid (DAPA) was analyzed. The unprotonated structures of these amino acids are shown below in Figure 3.1.

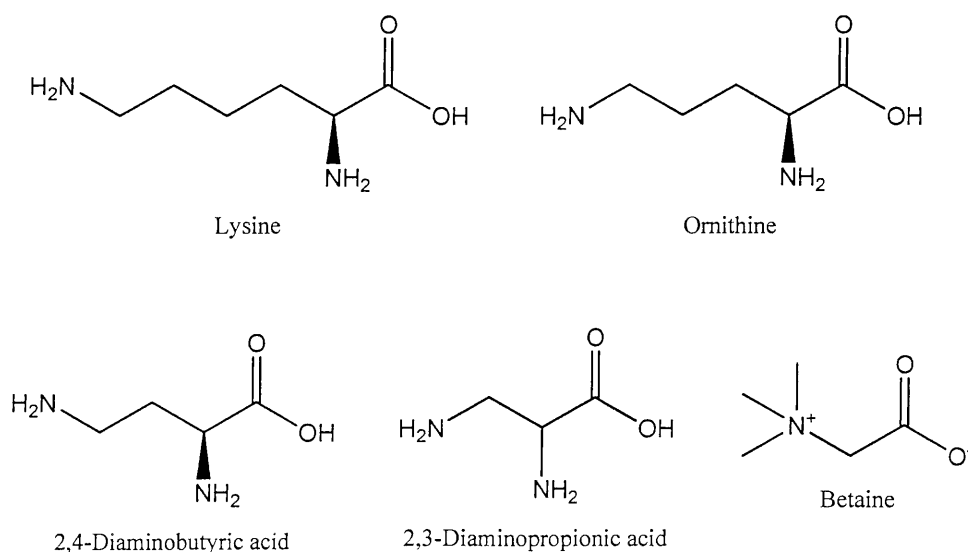


Figure 3.1 Structures of lysine, lysine's homologs, and betaine. The C-terminus of each amino acid is located on the right side of the structure, the N-terminus points downward, and the side chain extends from the  $\alpha$ -carbon to the left.

Amino acids were chosen for study because they are relatively simple polyfunctional compounds. The amino acids lysine, ornithine, DABA, and DAPA were chosen in particular because they are biologically relevant species. Although lysine is incorporated in proteins, its homologs ornithine, DABA, and DAPA, which differ only in the number of carbons in their side chains, are nonproteinogenic. Interestingly, while DAPA and DABA have been found as products in prebiotic syntheses, a prebiotic synthesis of ornithine and lysine has not been established.<sup>5</sup> It seems likely then that DAPA and DABA—and even ornithine—would have been higher in abundance than lysine during the early stages of evolution. It is not necessarily obvious why lysine was chosen for protein incorporation over its simpler counterparts. It may be that DAPA and DABA are more likely to undergo acyl migration when incorporated into peptide chains, making them unsuitable for protein synthesis. It is also possible that ornithine may halt protein synthesis by undergoing lactamization at the C-terminus.<sup>5</sup> Answering the complex question of why certain amino acids such as lysine are encoded for by the genetic code and why others are not is, of course, beyond the scope of this work. However, the above discussion shows why analysis of lysine, ornithine, DABA, and DAPA is important. By studying the H/D exchange behavior of these amino acids, it may be possible to gain insights into not only the H/D exchange process itself but also into the differences between compounds that seem very similar in terms of structure.

### 3.2 Experimental Procedures

The amino acids L-lysine (98% pure) and L-ornithine hydrochloride (99% pure) were obtained from Sigma. (S)-2,4-Diaminobutyric acid dihydrochloride (97% pure) and 2,3-diaminopropionic acid hydrochloride (98% pure) were obtained from Aldrich.

Betaine hydrochloride ( $\geq 99\%$  pure) was also purchased from Sigma. Solutions of the concentration  $5 \times 10^{-3}$  M were made of each compound in a 50:50 mix of HPLC grade methanol and purified water. After these stock solutions were sonicated, they were diluted to  $5 \times 10^{-5}$  M in clean vials with the same 50:50 mixture of methanol and water. Finally, glacial acetic acid from Fisher Scientific was pipetted into the dilute amino acid solutions at 1% of the solution volume.

All experiments were performed on the previously described (see Chapter 2) LCQ DECA ion trap mass spectrometer that had been modified to allow for the addition of a neutral reagent to the trap through the helium inlet system. A syringe pump was used with a 500  $\mu$ L syringe to leak liquid  $D_2O$  (Aldrich; 99.9% isotopic purity) into the helium inlet system at a flow rate of 400  $\mu$ L/hour throughout the course of the experiments. This slow flow rate made it possible for the helium to transport the  $D_2O$  to the trap. Before any amino acid samples were analyzed, the trap was “seasoned” with  $D_2O$  to try to limit back exchange.

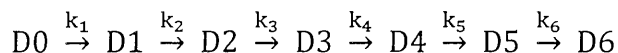
Once  $D_2O$  had been leaked into the trap for one to two hours, another syringe pump was used to introduce one of the  $5 \times 10^{-5}$  M amino acid solutions to the ESI source of the mass spectrometer at a flow rate of 800  $\mu$ L/hour. The helium regulator was set to 12 psi (83 kPa) so the bottom ball of the flow meter was at 24 to 28 with the flow meter being only partially open. This ensured that the flow meter could keep a steady flow of helium running to the ion trap. Next, the micro needle valve was opened to adjust the pressure at the ionization gauge, as indicated on the LCQ Tune instrument status panel. If the ion gauge pressure was too high, H/D exchange frequency increased, and it became difficult to observe the parent peaks. For example, although all of the exchanges of



ornithine could be observed at  $1.9 \times 10^{-5}$  Torr, this ion gauge pressure was too high to fully observe the decay of DAPA's parent peak. To correct the problem, the ion gauge pressure had to be lowered. When the ion gauge pressure was changed, the H/D exchange behavior of betaine (see Figure 3.1 for the structure of betaine) was also measured. After collecting spectra for all of the sample solutions at a variety of activation times as described in Chapter 2, the data was analyzed with Excel and the KinFit fitting routine.

### 3.3 Results

Lysine, ornithine, DABA, and DAPA have six possible exchange sites while betaine has only one possible exchange site. The ordinary differential equations used by KinFit to fit the data and extract rate constants were tailored to the number of possible exchanges. In addition, several fitting methods were applied to each data set; these methods included the simple fit, the  $^{13}\text{C}$  fit, and the back exchange fit. The simple and  $^{13}\text{C}$  fits both assumed that the parent ions (D0) underwent exchange to become the deuterated ions of the D1 peak. Then, the D1 ions underwent another exchange to become D2 ions, and so forth in a sequential manner such that



where  $k_1$  through  $k_6$  were the rate constants. When entered into KinFit the differential equations for analyzing the data of lysine and its homologs with the simple method were

$$\text{Ydot}(1) = -K1 * Y1$$

$$\text{Ydot}(2) = K1 * Y1 - K2 * Y2$$

$$\text{Ydot}(3) = K2 * Y2 - K3 * Y3$$

$$\text{Ydot}(4) = K3 * Y3 - K4 * Y4$$

$$Y_{\dot{5}} = K_4 * Y_4 - K_5 * Y_5$$

$$Y_{\dot{6}} = K_5 * Y_5 - K_6 * Y_6$$

$$Y_{\dot{7}} = K_6 * Y_6$$

where  $Y_{\dot{1}}$  was the relative abundance of the D0 ions, and so forth. The  $^{13}\text{C}$  method was similar except that it accounted for ions that were one mass unit heavier because they had incorporated a heavier isotope of carbon, nitrogen, or oxygen. The equations for this method took on the form

$$Y_{\dot{1}} = -K_1 * Y_1$$

$$Y_{\dot{2}} = K_1 * Y_1 - K_2 * (Y_2 - t_1 * Y_1)$$

$$Y_{\dot{3}} = K_2 * (Y_2 - t_1 * Y_1) - K_3 * (Y_3 - t_1 * Y_2)$$

$$Y_{\dot{4}} = K_3 * (Y_3 - t_1 * Y_2) - K_4 * (Y_4 - t_1 * Y_3)$$

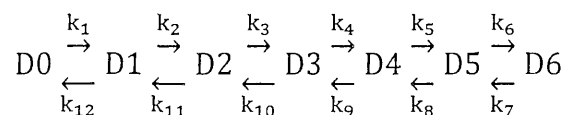
$$Y_{\dot{5}} = K_4 * (Y_4 - t_1 * Y_3) - K_5 * (Y_5 - t_1 * Y_4)$$

$$Y_{\dot{6}} = K_5 * (Y_5 - t_1 * Y_4) - K_6 * (Y_6 - t_1 * Y_5)$$

$$Y_{\dot{7}} = K_6 * (Y_6 - t_1 * Y_5)$$

where  $t_1$  was obtained from an isotope pattern calculator and represented the relative size of the peak that would be approximately one mass unit higher due to isotope incorporation.

Unlike the previous fitting routines, the back exchange method assumed that ions could undergo exchange reactions to gain deuterium atoms as well as exchange reactions to lose deuterium atoms. Both the forward and back exchanges were governed by rate constants such that



Thus, the equations for analyzing the H/D exchange kinetics of lysine and its homologs with the back exchange method were

$$Y_{\text{dot}}(1) = -K1 * Y1 + K12 * Y2$$

$$Y_{\text{dot}}(2) = K1 * Y1 + K11 * Y3 - (K2 + K12) * Y2$$

$$Y_{\text{dot}}(3) = K2 * Y2 + K10 * Y4 - (K3 + K11) * Y3$$

$$Y_{\text{dot}}(4) = K3 * Y3 + K9 * Y5 - (K4 + K10) * Y4$$

$$Y_{\text{dot}}(5) = K4 * Y4 + K8 * Y6 - (K5 + K9) * Y5$$

$$Y_{\text{dot}}(6) = K5 * Y5 + K7 * Y7 - (K6 + K8) * Y6$$

$$Y_{\text{dot}}(7) = K6 * Y6 - K7 * Y7$$

Finally, the exchange data of betaine was fit with the appropriate method and number of equations. It was possible to obtain the concentration of D<sub>2</sub>O in the trap by dividing the relative rate coefficient given by KinFit by the absolute rate coefficient (1.00 x 10<sup>-12</sup> cm<sup>3</sup> molecule<sup>-1</sup> s<sup>-1</sup>) of betaine's single, well-characterized exchange.<sup>3</sup> The absolute forward rate coefficients for lysine and its homologs were calculated by dividing their relative rate coefficients by the concentration of D<sub>2</sub>O in the trap on the day of the experiment.

Lysine, ornithine, DABA, and DAPA were observed to exchange all six of their labile hydrogen atoms during the course of the experiments (see Figure 3.2 for sample mass spectra). Three plots produced by KinFit showing the normalized peak intensity data for DABA in comparison to the curves predicted by the simple, <sup>13</sup>C, and back exchange methods are also shown in Figure 3.3. A side-by-side comparison demonstrates

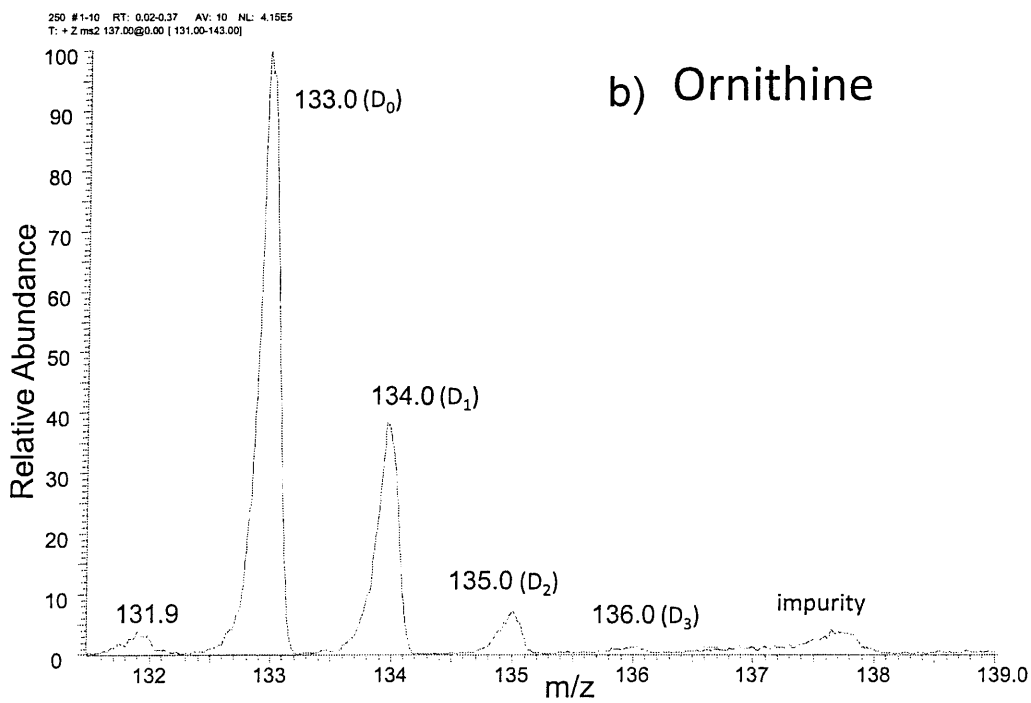
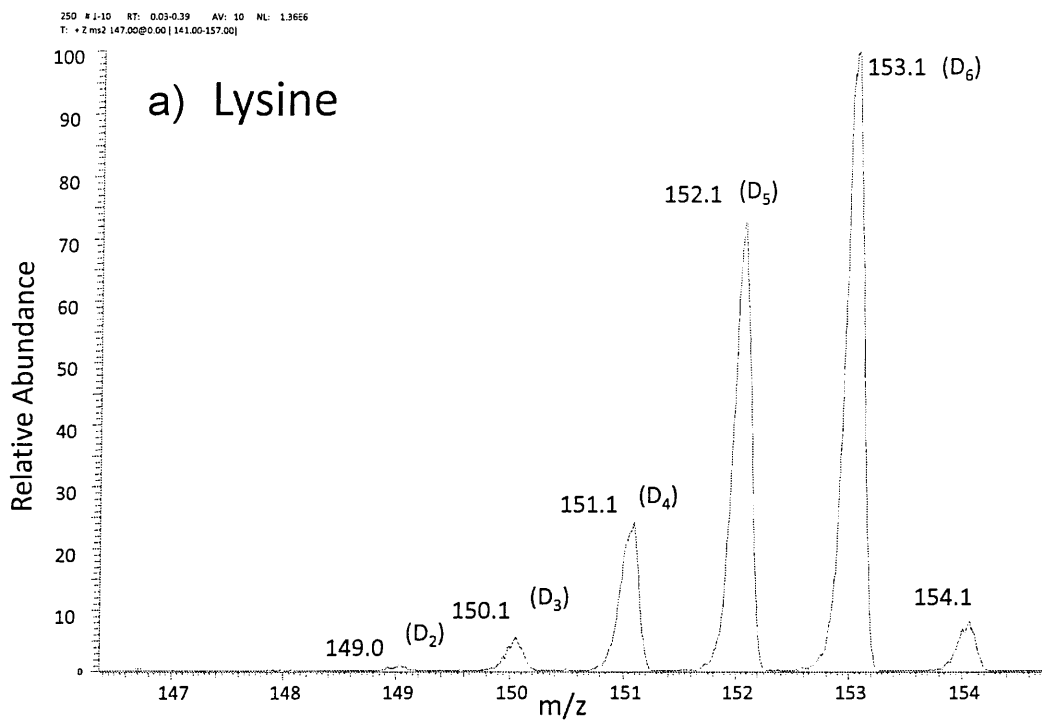


Figure 3.2 a, b Mass spectra for protonated lysine and ornithine under H/D exchange conditions at a reaction time of 250 ms and an ion gauge pressure of approximately  $1.9 \times 10^{-5}$  Torr

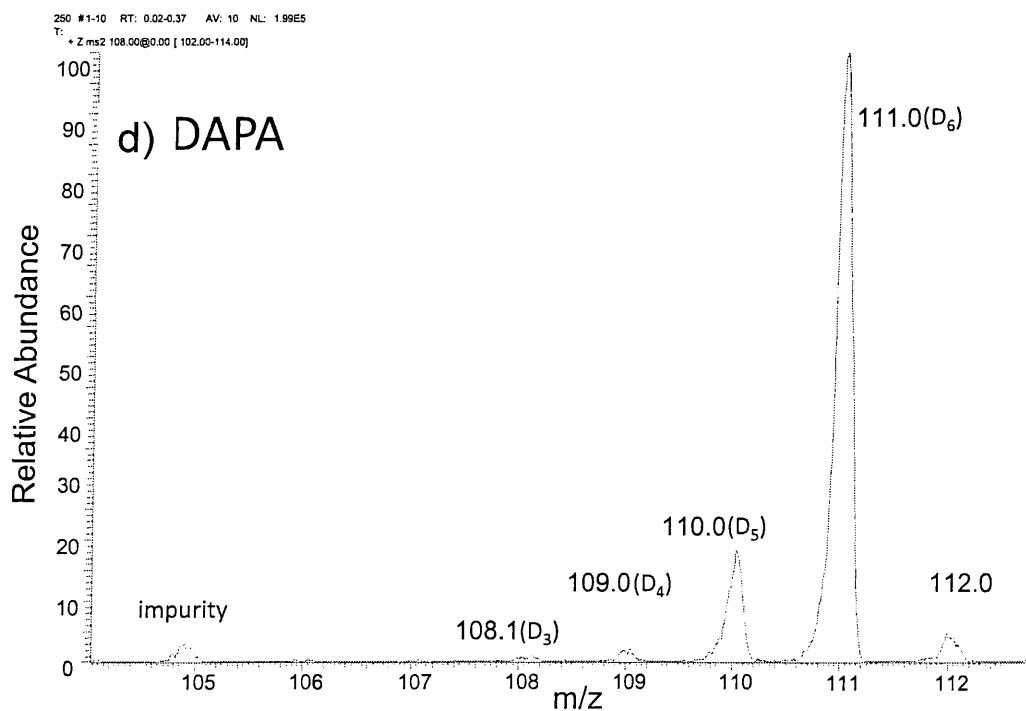
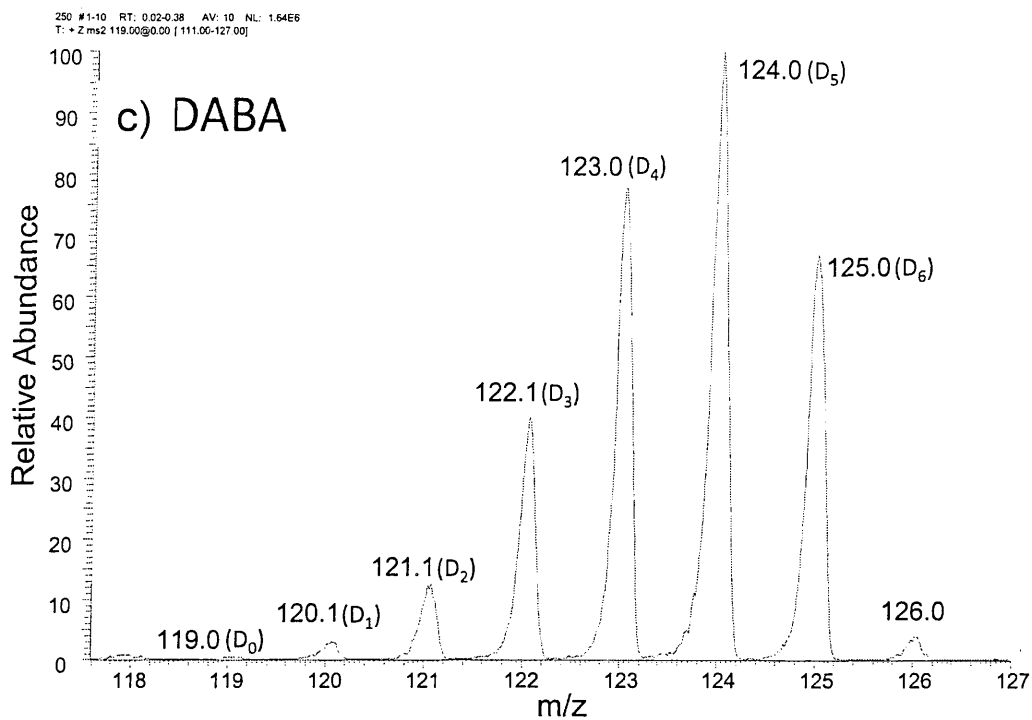


Figure 3.2 c, d Mass spectra for protonated DABA and DAPA under H/D exchange conditions at a reaction time of 250 ms and an ion gauge pressure of approximately  $1.9 \times 10^{-5}$  Torr

that the back exchange method most accurately represented the H/D exchange kinetics for DABA. Although the plots for lysine, ornithine, and DAPA are not shown here, the same three methods were used to analyze the H/D exchange behavior of each amino acid, and it was found that the back exchange method provided the best fit in all cases.

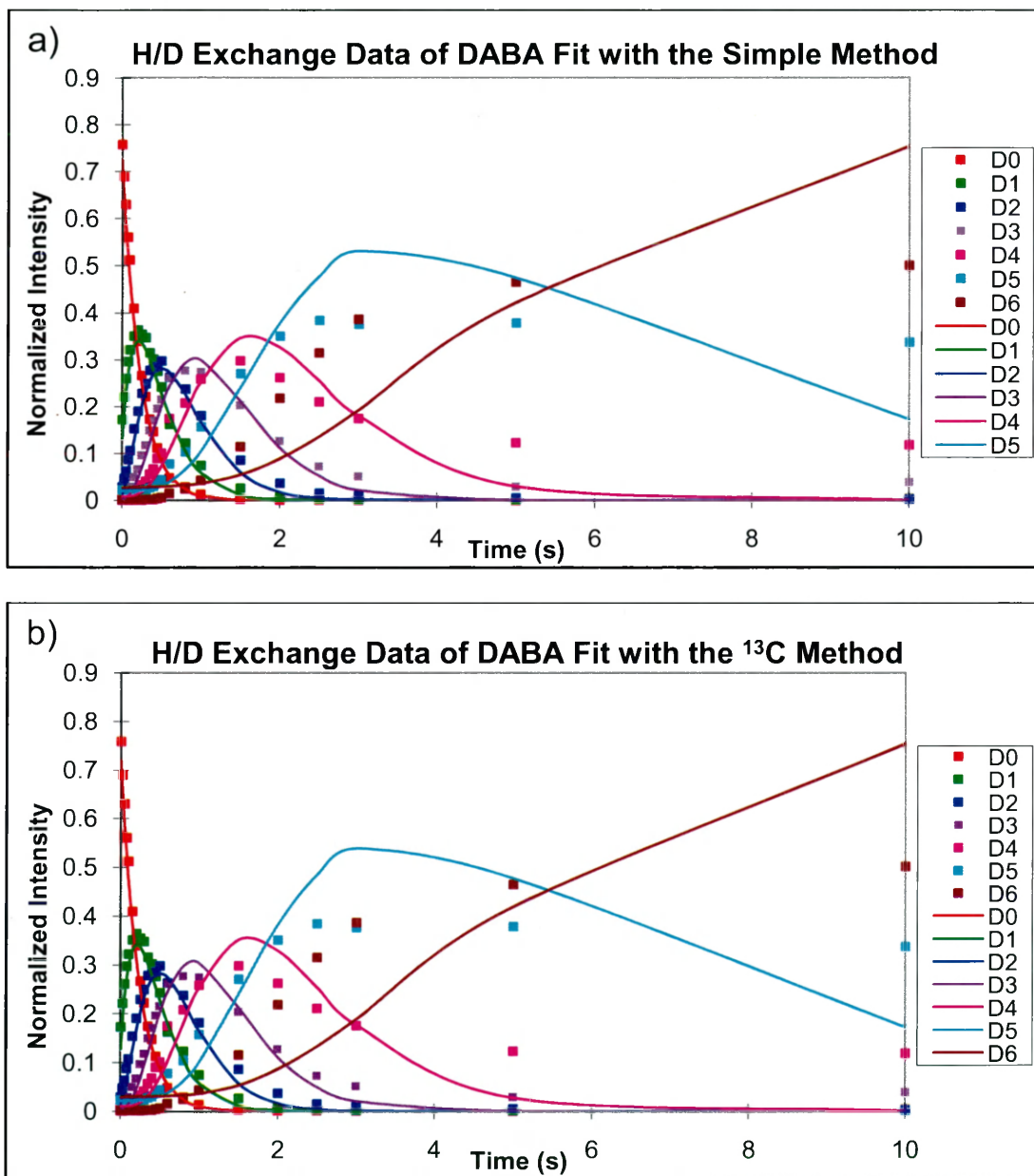


Figure 3.3 a,b Simple and <sup>13</sup>C fits done with KinFit. The squares represent experimental data and the solid curves represent the theoretical fits of the ODEs

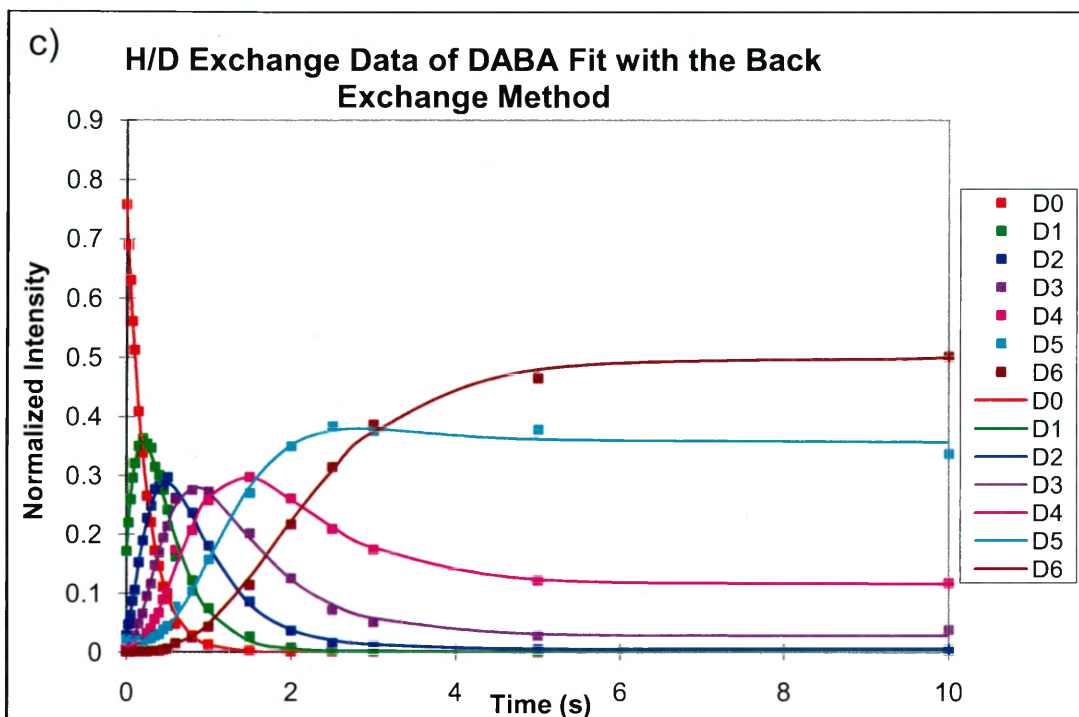


Figure 3.3 c Back exchange fit done with KinFit. The squares represent experimental data and the solid curves represent the theoretical fits of the ODEs

In general, lysine, ornithine, DABA, and DAPA have three relatively fast exchanges, two slightly slower exchanges, and one much slower exchange. Despite this overall trend, the absolute rate coefficients for the exchanges vary among the amino acids. Table 3.1 shows the six absolute rate coefficients for lysine, ornithine, DABA, and DAPA. Each value in the table is the average of three to four trials and is reported with

|      | $k_1$            | $k_2$            | $k_3$            | $k_4$            | $k_5$            | $k_6$            |
|------|------------------|------------------|------------------|------------------|------------------|------------------|
| Lys  | $12.5 \pm 14\%$  | $10.8 \pm 20\%$  | $9.15 \pm 15\%$  | $6.93 \pm 11\%$  | $4.80 \pm 10\%$  | $2.40 \pm 9.3\%$ |
| Orn  | 0.475            | 0.405            | 0.348            | 0.268            | 0.189            | 0.131            |
| DABA | $7.44 \pm 9.9\%$ | $7.07 \pm 9.1\%$ | $6.69 \pm 8.0\%$ | $5.47 \pm 13\%$  | $3.94 \pm 22\%$  | $2.19 \pm 19\%$  |
| DAPA | $27.5 \pm 14\%$  | $24.8 \pm 4.5\%$ | $21.2 \pm 6.4\%$ | $16.4 \pm 7.4\%$ | $11.0 \pm 5.6\%$ | $5.42 \pm 3.5\%$ |

\*Rate coefficients are presented as  $k \times 10^{-11} \text{ cm}^3 \text{ molecule}^{-1} \text{ s}^{-1}$

its relative standard deviation, except in the case of ornithine, whose value is the average of only two trials. As previously mentioned, these trials were conducted at different ion gauge pressures, usually in the range of  $1.3 \times 10^{-5}$  to  $1.9 \times 10^{-5}$  Torr. However, because the single exchange of betaine—and thus the  $D_2O$  concentration in the trap—was measured at each ion gauge pressure, these numbers can be compared to one another. This estimation of the concentration of  $D_2O$  in the trap from the relative rate constant of betaine is also the largest source of error in the experiments. The literature value for betaine's rate constant has an error of approximately 20% due to estimations of background pressure in the ICR cell.<sup>3</sup> Therefore, the absolute error for the rate constants presented here can be no smaller than 20% and is probably closer to 30%.

### 3.4 Discussion

In agreement with a previous study involving H/D exchange of protonated lysine with  $CH_3OD$  and  $D_2O$ ,<sup>6</sup> protonated lysine in the current study was shown to exchange all of its labile hydrogen atoms. Rožman and co-workers described 5 equivalent rate constants of  $9.5 \times 10^{-11} \text{ cm}^3 \text{ molecules}^{-1} \text{ s}^{-1}$  and one slower rate constant of  $4.4 \times 10^{-11} \text{ cm}^3 \text{ molecules}^{-1} \text{ s}^{-1}$  for the 6 exchanges of lysine.<sup>6</sup> Although the rate coefficients given here are on the same order of magnitude as those found previously, the first five rate coefficients for lysine in this study were not found to be approximately the same. This discrepancy likely occurs because the rate coefficients reported by Rožman and co-workers are site-specific rate constants. The rate coefficients calculated via KinFit, however, are not site-specific. Therefore, while the researchers who conducted the previous study concluded that the five equivalent rate constants corresponded to exchanges of the hydrogens on the N-terminus and side chain and that the slower rate

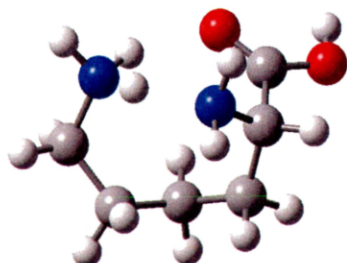


constant represented exchange at the carboxylic acid of lysine,<sup>6</sup> no such generalizations can be made here. As Campbell and co-workers point out, it is tempting to think that early H/D exchange occurs at the most reactive site.<sup>3</sup> However, in this case, the first exchanges do not necessarily occur at only one site. In other words, the D1 peak in the mass spectrum is composed of ions that have been deuterated at a variety of sites so  $k_1$  actually “represents the sum of the rate constants for each individual D1 species and gives the total rate for reaction at all sites.”<sup>3</sup>

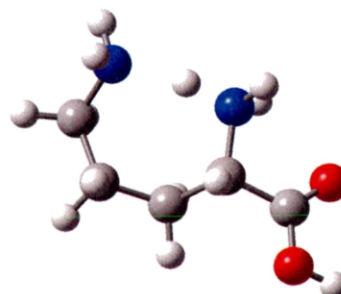
If it is not possible to deduce which rate coefficients correspond to which exchanges from the data and calculations already presented, then the focus needs to shift to what can be learned through comparisons of lysine, ornithine, DABA, and DAPA. For instance, ornithine stands out from the other compounds in the study because its exchanges are by far the slowest even though it has the second longest side chain. It may be that protonated ornithine is in a vastly different conformation in the gas phase when compared to the structures of protonated lysine, DABA, and DAPA. However, calculations at the B3LYP level of theory with the 6-31 +G\*\* basis set suggest that this is not true. The lowest energy structures of protonated lysine and its homologs presented in Figure 3.4 are remarkably similar to one another because the N-terminus is involved in a hydrogen bond with the side chain in each case.

Since the structures of protonated lysine, ornithine, DABA, and DAPA are similar, the differences in H/D exchange rates among the compounds may be due to differences in energy barriers for the exchanges themselves. Because D<sub>2</sub>O is a less basic deuterating agent than methanol or ammonia, the exchange of the C-terminus hydrogen is proposed to occur via a flip-flop mechanism, and the exchanges at the N-terminus and

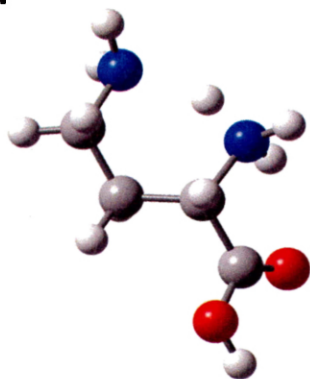
LysH<sup>+</sup>



OrnH<sup>+</sup>



DABAH<sup>+</sup>



DAPAH<sup>+</sup>

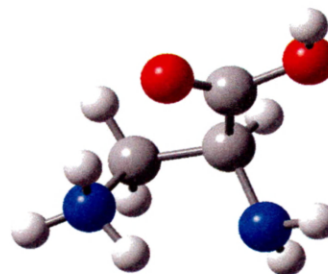


Figure 3.4 The lowest energy structures presented above for protonated lysine, ornithine, DABA, and DAPA were obtained at the B3LYP level of theory with the 6-31+G\*\* basis set. In these ball and stick figures, carbon atoms are dark grey, oxygen atoms are red, nitrogen atoms are blue, and hydrogen atoms are light grey.

side chain are proposed to take place through a relay mechanism<sup>3</sup> (see Chapter 1 for further details on exchange mechanisms). Interactions of D<sub>2</sub>O with protonated ornithine, DABA, and DAPA were also modeled at B3LYP/6-31+G\*\*. In these calculations, a water molecule was placed at different points around the amino acid to simulate the initiation of either the relay or flip-flop exchange mechanism; these structures were optimized, transition states were found, and the barriers to each exchange mechanism were calculated. Table 3.2 below summarizes the barriers to exchange for each of the compounds. Figure 3.5 is a potential energy surface for the exchange reactions of protonated DAPA and presents a more holistic view of how these amino acids interact with D<sub>2</sub>O or water when undergoing exchange.

| Table 3.2 Calculated barriers to H/D exchange mechanisms for protonated lysine and its homologs |                              |                          |
|---|------------------------------|--------------------------|
|   | Flip-flop Barrier (kcal/mol) | Relay Barrier (kcal/mol) |
| Ornithine   | 13.8                         | 10.5                     |
| DABA  | 12.6                         | 6.7                      |
| DAPA  | 13.0                         | 8.6                      |

As indicated by the values reported in the table above, the barriers for exchange at the carboxylic acid via the flip-flop mechanism or between nitrogen atoms via a relay mechanism are very similar for ornithine, DABA, and DAPA. Therefore, it seems unlikely that the energy needed to overcome these barriers for exchange to occur is what causes the rate coefficients of ornithine to be so low. It is possible that there is a large energy barrier for the water molecule to move from its position in the global minimum structure to a position in which it can initiate exchange, but the global minima for protonated ornithine, DABA, and DAPA interacting with water have not yet been found. Thus, future work could consist of searching for these global minima and calculating the

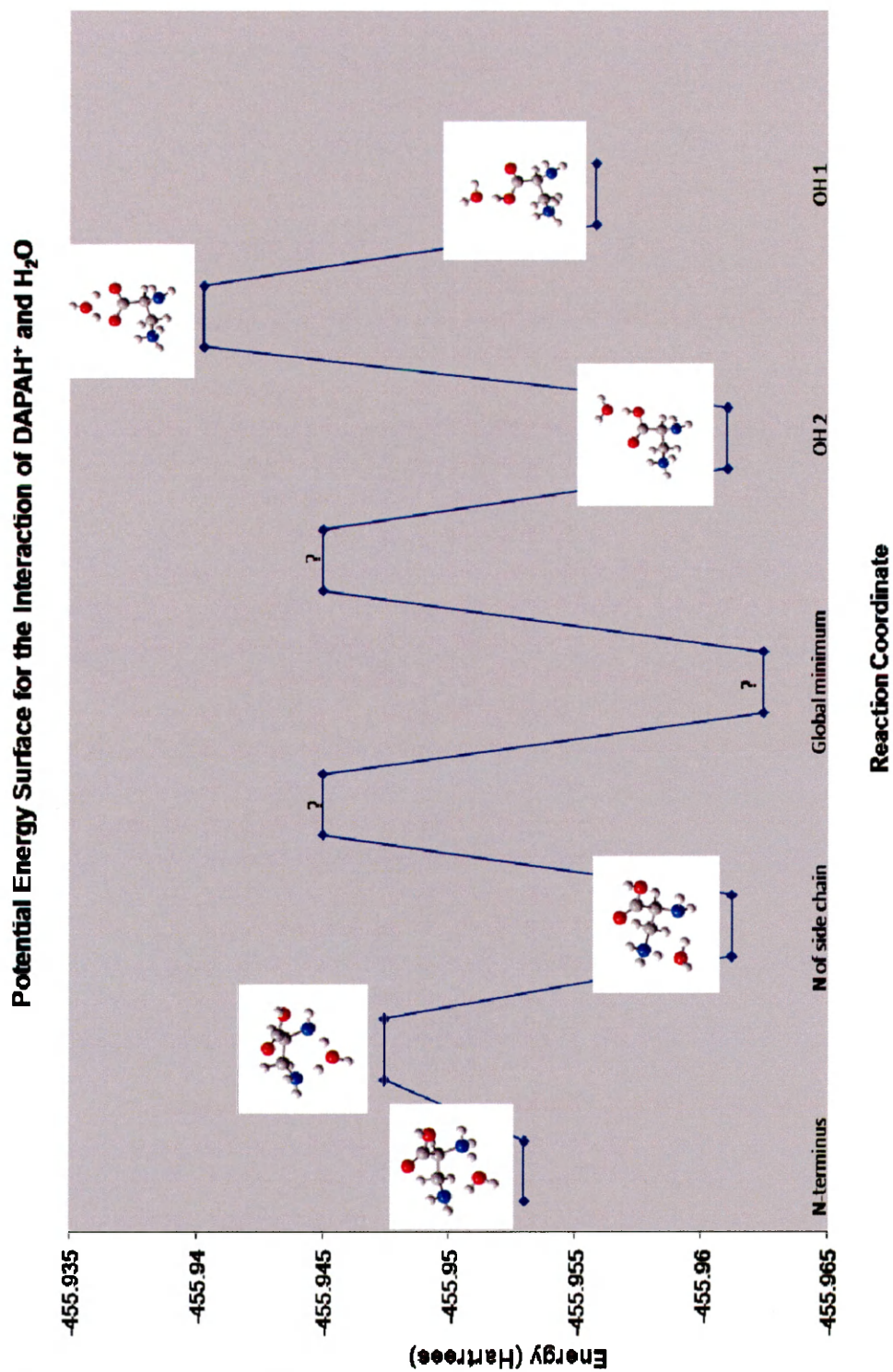


Figure 3.5 PES for the interaction of water with protonated DAPA. The location of the water molecule is listed along the reaction coordinate. The lowest energy structures were obtained with B3LYP/6-31+G\*\*

amount of energy needed for the water to move from its global minimum to begin exchange. It would also be worthwhile to re-examine the fitting practices used throughout. When fitting experimental data for lysine and its homologs, the system was treated as a series of successive exchanges. This produces “apparent” rate constants for the transition of a D0 ion to a D1 ion, and so on, regardless of where the exchanges are actually taking place. It may be more accurate to treat D1 as a sum of all the possible ion species in which one deuterium has been incorporated; this can be accomplished through a site-specific analysis. Several site-specific approaches in which each site of exchange is assumed to have its own rate coefficient have already been described.<sup>1,6-8</sup> Some site-specific approaches utilize the Runge-Kutta method in commercially available programs such as Mathematica.<sup>1</sup> Others use a stand-alone program that requires initial guesses of the rate constants and the “stiffness” of the system. The program then iteratively solves the differential equations until the variance between the experimental data and theoretical fit is below a specified level.<sup>8</sup> No matter which approach is used, being able to obtain site-specific rate coefficients would greatly enhance our understanding of the H/D exchange process. It would also make it significantly easier to compare results with other studies.

### 3.5 References

1. Gard, E.; Willard, D.; Bregar, J.; Green, M. K.; Lebrilla, C. B. *Org. Mass Spectrom.* **1993**, *28*, 1632-1639.
2. Ausloos, P.; Lias, S. G. *J. Am. Chem. Soc.* **1981**, *103*, 3641-3647.
3. Campbell, S.; Rodgers, M. T.; Marzluff, E. M.; Beauchamp, J. L. *J. Am. Chem. Soc.* **1995**, *117*, 12840-12854.
4. Cheng, X.; Feneslau, C. *Int. J. Mass Spectrom. Ion Processes* **1992**, *122*, 109-119.

5. Weber, A. L.; Miller, S. L. *J. Mol. Evol.* **1981**, *17*, 273-284.
6. Rožman, M.; Srzić, D.; Klasinc, L. *Int. J. Mass Spectrom.* **2006**, *253*, 201-206.
7. Rožman, M.; Kazazić, S.; Klasinc, L.; Srzić, D. *Rapid Commun. Mass Spectrom.* **2003**, *17*, 2769-2772.
8. He, F.; Marshall, A. G. *J. Phys. Chem. A* **2000**, *104*, 562-567.

## Chapter 4: H/D Exchange Behavior of Arginine and Canavanine

### 4.1 Introduction

Amino acids are polyfunctional compounds that are known to exist as zwitterions in aqueous solution.<sup>1</sup> Zwitterions can have negative and positive charges at certain locations, but they do not have a net charge. For amino acids in solution, it is often the case that the carboxylic acid at the C-terminus protonates the basic amino group at the N-terminus; this means that the deprotonated carboxyl group carries a negative charge and the protonated amino group carries a positive charge while the molecule as a whole is neutral (see Figure 4.1).

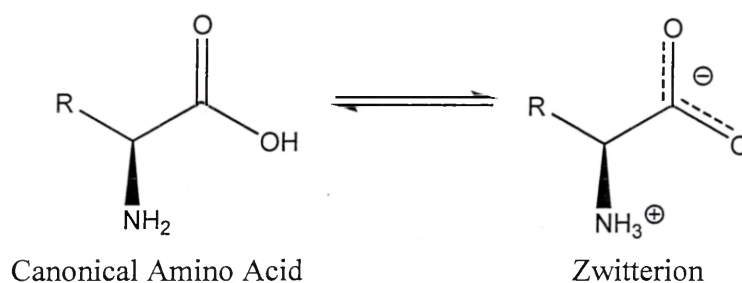


Figure 4.1 Conversion of a generic amino acid into its corresponding zwitterion

Despite the fact that this phenomenon is well documented in the solution phase, there has been debate over whether amino acids retain their zwitterionic character when there is no solvent present. Analysis of the gas phase acidity and basicity of the amino acid glycine using Fourier transform-ion cyclotron resonance mass spectrometry indicates that glycine does not exist as a zwitterion in the gas phase.<sup>2</sup> Ab initio calculations also show that the glycine zwitterion is less stable than its neutral counterpart in the gas phase by approximately 16 to 20 kcal/mol.<sup>1</sup> Furthermore, while theoretical calculations show that

as few as two water molecules can stabilize the glycine zwitterion,<sup>1,2</sup> experimental results indicate that five water molecules are needed.<sup>2</sup>

Arginine is the most basic amino acid, and as such, it is also the most likely to exist as a zwitterion in the gas phase. Its high basicity can help stabilize the zwitterionic form in comparison to other amino acids.<sup>2</sup> In a short communication, Price and co-workers detailed how their theoretical calculations indicated that the most energetically favorable form of arginine in the gas phase was a zwitterion in which the C-terminus was deprotonated and the guanidinium group of the side chain was protonated. However, they noted that the lowest energy structure of the neutral molecule may not have been found and that they would need to perform calculations at a higher level of theory for confirmation.<sup>1</sup> Cavity ring-down experiments done since then have indeed shown that arginine does not exist as a zwitterion by itself, although the zwitterionic form of arginine can be stabilized by noncovalent interactions with other molecules and ions.<sup>2</sup> For example, large alkali metal cations can stabilize the arginine zwitterion in the gas phase to form a salt-bridge complex.<sup>3</sup> In addition, experimental studies of the dissociation kinetics of proton-bound dimers indicate that the proton-bound arginine homodimer exists as a salt-bridge complex in the gas phase.<sup>1</sup> Theoretical studies involving molecular mechanics and density functional theory are in agreement. The most stable conformation of the arginine dimer is a salt-bridge form in which one arginine is protonated on its side chain and the other arginine is a zwitterion.<sup>4</sup>

Arginine is an interesting case for analysis with H/D exchange because it can exist in different forms depending on whether it is a monomer or dimer in the gas phase.





### I Salt Bridge

Figure 4.2 Salt bridge structure of the proton-bound arginine dimer. The arginine on the left is a zwitterion, and the arginine on the right is a protonated ion. Taken from Strittmatter and Williams<sup>4</sup>

Canavanine is another interesting possibility for study with H/D exchange because it is a nonproteinogenic but still biologically relevant homolog of arginine. The structures of canavanine and arginine are similar except that canavanine contains an oxygen atom in place of the last methylene group in the amino acid side chain.<sup>5</sup> This oxygen substitution lowers the absolute PA of canavanine by approximately 9 to 12 kcal/mol in comparison to arginine.<sup>6</sup> However, the structural similarities between canavanine and arginine allow canavanine to act “in virtually every enzyme-mediated reaction that preferentially employs arginine as a substrate,” including the charging of the tRNA of arginine with canavanine by the arginyl tRNA synthetase.<sup>5</sup>

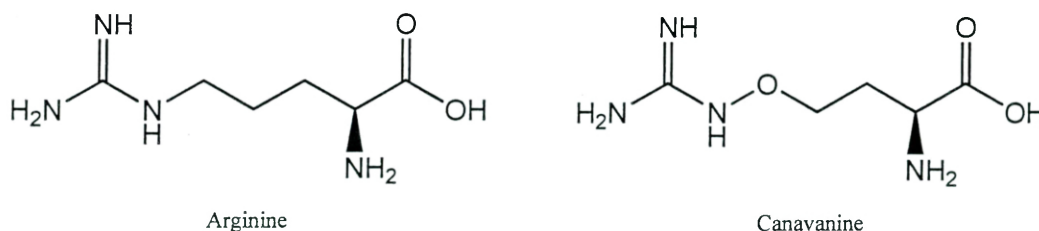


Figure 4.3 Comparison of arginine and canavanine. Oxygen substitution takes place at the  $\delta$ -methylene group of the arginine side chain.

Canavanine is produced by certain leguminous plants and is often stored in the seeds. Besides serving as a nitrogen supply, the non-protein oxyanalog of arginine provides these plants with a defense mechanism because canavanine-sensitive insects cannot differentiate between canavanine and arginine.<sup>5</sup> Misincorporation of canavanine in proteins can result in changes in basicity or hydrogen bonding that cause newly synthesized insect proteins to be abnormal in structure and function.<sup>6</sup> Other insects that regularly feed on seeds containing canavanine, however, have developed arginyl tRNA synthetases that can discriminate between canavanine and arginine, which prevents misincorporation in proteins.<sup>5</sup> Elucidating why some arginyl tRNA synthetases discriminate between canavanine and arginine and why others do not may be aided by a deeper understanding of the structure and properties of canavanine. Comparison of the H/D exchange behavior of canavanine and arginine may provide new insights into the structures of these molecules.

#### 4.2 Experimental Procedures

L-Arginine ( $\geq 98\%$  pure) was obtained from Aldrich, and L-canavanine from the Jack bean *Canavalia ensiformis* ( $\geq 98\%$  pure) was obtained from Sigma. Stock solutions and sample solutions of arginine and canavanine were prepared using the procedure outlined in the Chapter 3. The only difference in procedure was that the ratio of acetic acid added to the sample solutions was increased to 5% of the solution volume in some cases to promote dimerization. The H/D exchange behavior of arginine and canavanine was examined with the modified LCQ DECA ion trap mass spectrometer, as outlined in Chapter 2. The monomeric forms of the compounds were studied at ion gauge pressures between  $1.7 \times 10^{-5}$  and  $1.9 \times 10^{-5}$  Torr; the proton-bound homodimers of arginine and

canavanine were analyzed at  $1.2 \times 10^{-5}$  to  $1.3 \times 10^{-5}$  Torr. Finally, relative rate coefficients for the exchange reactions were obtained with KinFit and the back exchange method when possible. As explained in Chapter 3, the equations used by KinFit were modified to account for all of the possible exchanges.

### 4.3 Results

The protonated monomeric form of canavanine was observed to exchange all eight of its labile hydrogen atoms during three separate analyses. Relative rate coefficients for these exchanges were obtained with KinFit and the back exchange method, and three separate runs of betaine were used to calculate concentration of  $D_2O$  in the trap so the absolute rate coefficients could also be calculated. In order from  $k_1$  to  $k_8$  the average absolute rate coefficients for canavanine in units of  $k \times 10^{-11} \text{ cm}^3 \text{ molecule}^{-1} \text{ s}^{-1}$  are  $2.81 \pm 5.3\%$ ,  $2.55 \pm 3.1\%$ ,  $2.27 \pm 3.3\%$ ,  $1.91 \pm 8.2\%$ ,  $1.63 \pm 7.2\%$ ,  $1.26 \pm 6.2\%$ ,  $0.832 \pm 5.1\%$ , and  $0.482 \pm 4.5\%$ . In contrast, protonated monomeric arginine did not undergo significant exchange under the experimental conditions, so rate constants could not be calculated. The mass spectra of the canavanine and arginine monomers shown below in Figure 4.4 highlight the difference in their reactivities with  $D_2O$ . The primary peak in the mass spectrum of canavanine at an activation time of 2 seconds and an ion gauge pressure of  $1.9 \times 10^{-5}$  Torr is the D7 peak at  $m/z$  184.1. The primary peak in the mass spectrum of arginine at the same activation time and ion gauge pressure is the D0 peak at  $m/z$  175.1.

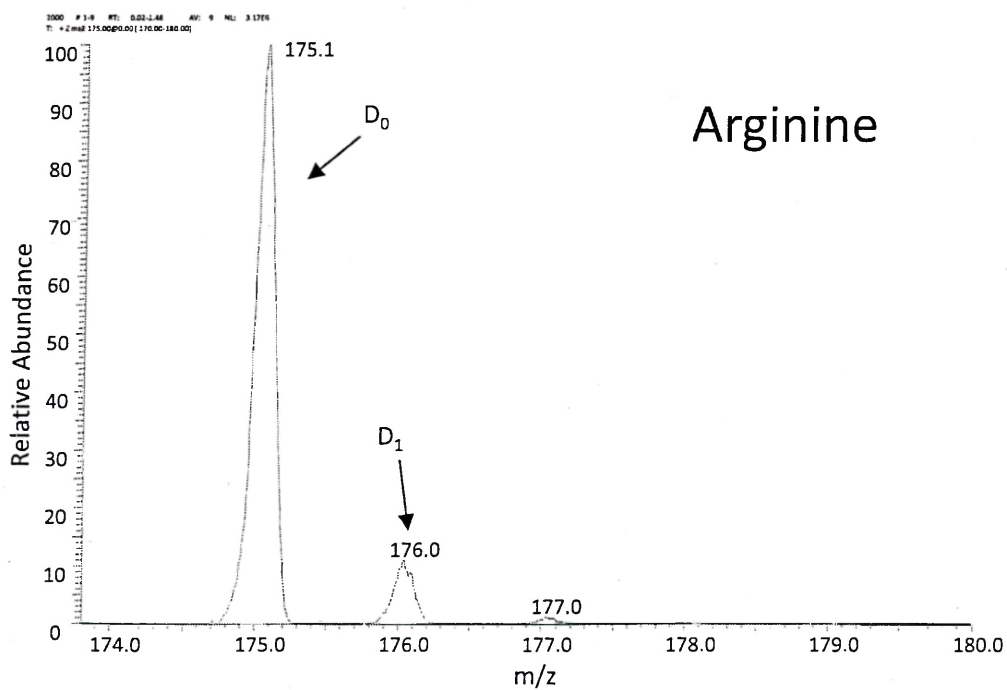
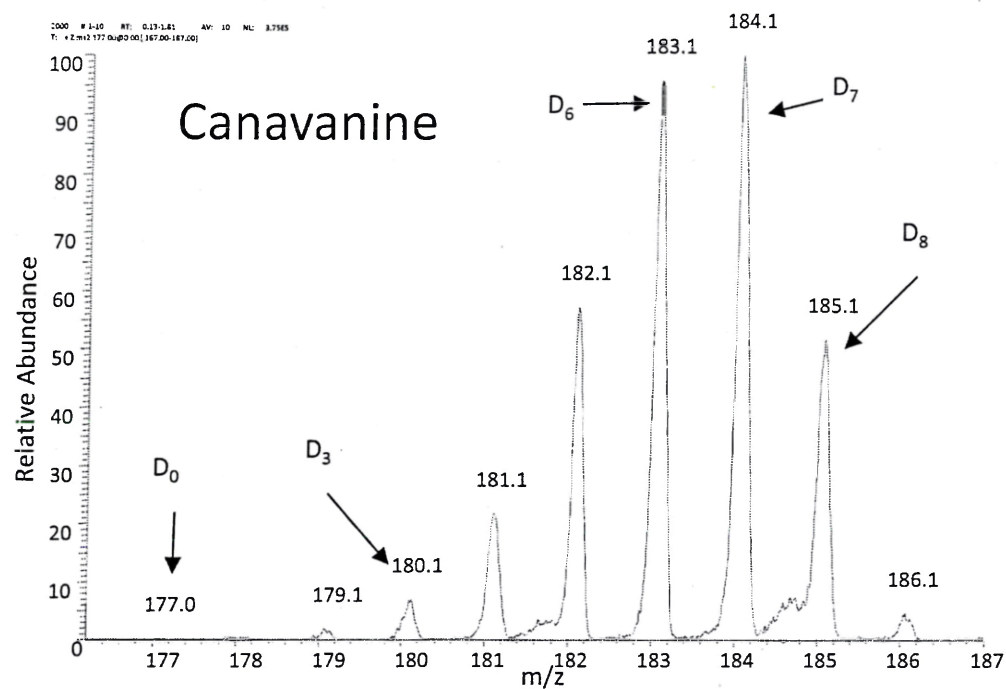


Figure 4.4 Mass spectra for protonated canavanine and arginine under H/D exchange conditions. Both spectra were collected on the same day at a reaction time of 2 s and an ion gauge pressure of  $1.9 \times 10^{-5}$  Torr

The proton-bound dimers of canavanine and arginine were observed to exchange all 15 of their labile hydrogen atoms, albeit at different rates. Again, the back exchange method was used to obtain relative rate coefficients for the exchanges. It was possible to obtain absolute rate coefficients for the analysis of canavanine and arginine dimers that occurred at an ion gauge pressure of approximately  $1.2 \times 10^{-5}$  Torr by fitting betaine data, but this was not possible for the analysis of the dimers that was completed at an ion gauge pressure of  $1.3 \times 10^{-5}$  Torr. Thus, only the average of the relative rate constants collected on two different days is reported in Table 4.1. The primary source of error in these experiments is the estimation of the concentration of  $D_2O$  in the trap according to the rate coefficient of betaine. Since the relative standard deviation for the previous canavanine and arginine experiments was less than 20% for each absolute rate constant and the relative rates reported in Table 4.1 do not make use of betaine, the error for the relative rate coefficients of the dimers is estimated to be 20% or lower.

| Table 4.1 Relative rate coefficients for the H/D exchange of two proton-bound dimers |                  |                |
|--|------------------|----------------|
|  | Canavanine Dimer | Arginine Dimer |
| $k_1$  | 2.50             | 8.97           |
| $k_2$  | 2.48             | 8.71           |
| $k_3$  | 2.14             | 8.14           |
| $k_4$  | 2.19             | 7.43           |
| $k_5$  | 2.04             | 6.96           |
| $k_6$  | 1.93             | 6.58           |
| $k_7$  | 1.80             | 6.83           |
| $k_8$  | 1.62             | 6.68           |
| $k_9$  | 1.66             | 6.00           |
| $k_{10}$   | 1.32             | 5.29           |
| $k_{11}$   | 1.31             | 4.79           |
| $k_{12}$   | 0.973            | 3.90           |
| $k_{13}$   | 0.885            | 2.73           |
| $k_{14}$   | 0.752            | 1.74           |
| $k_{15}$   | 0.167            | 0.927          |

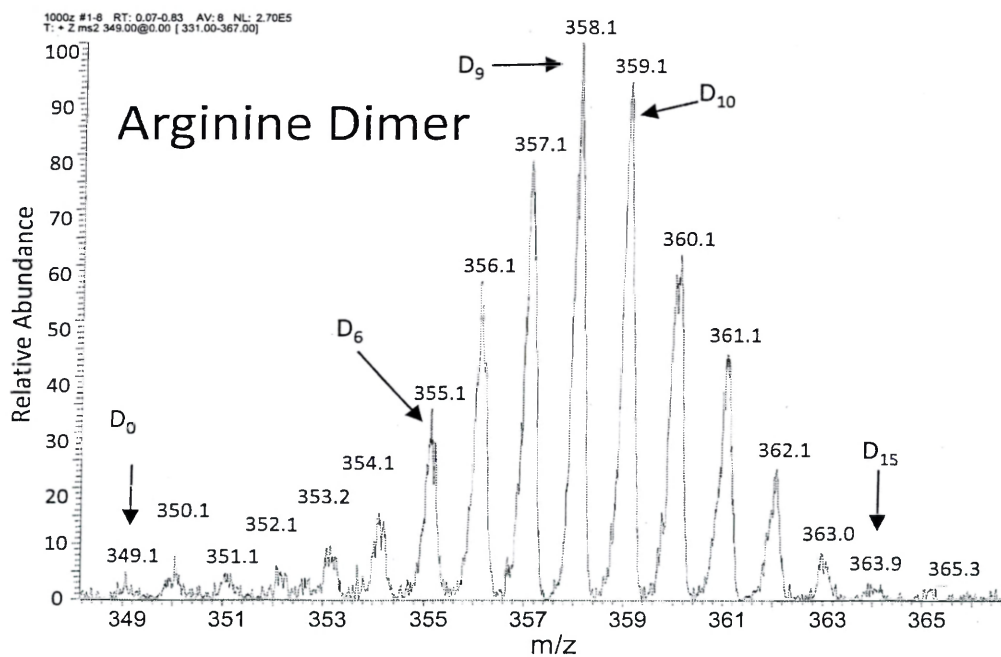
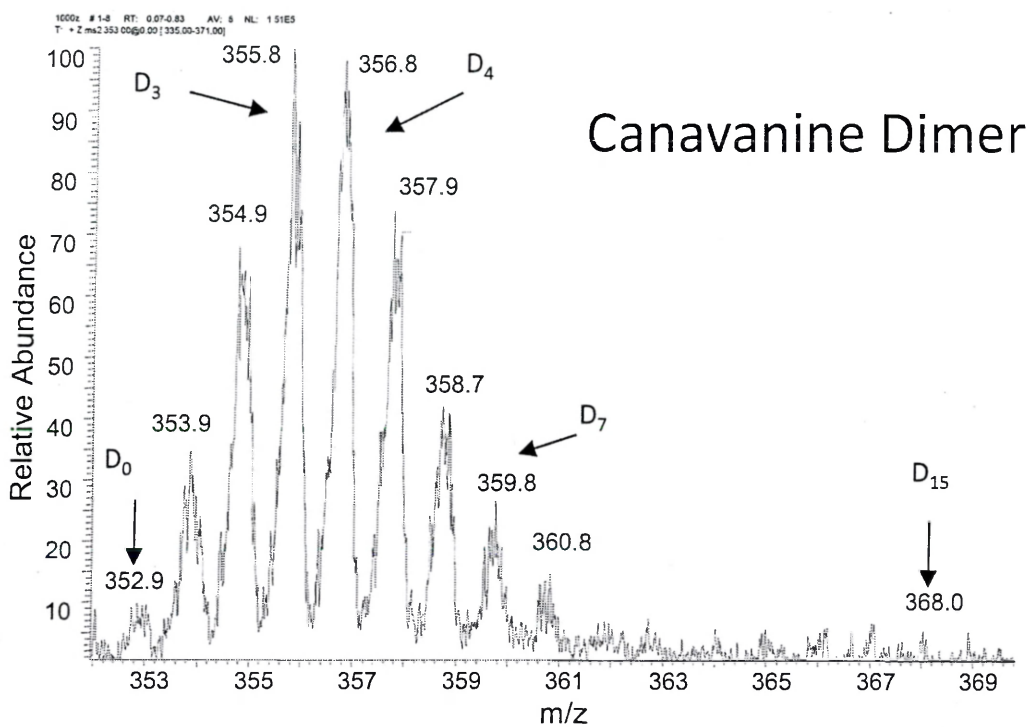


Figure 4.5 Mass spectra of the proton-bound dimers of canavanine and arginine. Both spectra were collected on the same day at a reaction time of 1 s and an ion gauge pressure of  $2.1 \times 10^{-5}$  Torr.

As before, canavanine and arginine display different H/D exchange behavior. In the case of the dimers, however, arginine appears to undergo exchange much more quickly than canavanine; the relative rate constants for the proton-bound arginine dimer are at least twice as large as those of the canavanine dimer. This trend is also apparent in the mass spectra of the proton-bound dimers. For example, the H/D exchange of dimeric canavanine is represented in the first mass spectrum of Figure 4.5 above. At an activation time of 1 s, the largest peaks are the D3 and D4 peaks at  $m/z$  355.8 and 356.8, respectively. The exchange of the arginine dimer at the same activation time is represented in the second mass spectrum of Figure 4.5; here, the D9 peak at  $m/z$  358.1 is the primary peak.

#### 4.4 Discussion

The protonated arginine monomer was not observed to undergo significant H/D exchange in this study although protonated arginine has eight possible exchange sites. The lack of exchange for the arginine monomer is in good agreement with previous studies.<sup>7,8</sup> For instance, Geller and Lifshitz report observing only 3 relatively large exchange peaks and 3 more very small exchange peaks when they reacted protonated arginine with  $\text{ND}_3$  in their electrospray ionization-fast flow quadrupole mass spectrometer.<sup>8</sup> It is not surprising that even the three obvious exchanges reported by Geller and Lifshitz are absent in the current study because  $\text{D}_2\text{O}$  is much less basic than  $\text{ND}_3$ . A large PA difference between the compound of interest and the deuterating reagent inhibits H/D exchange. The reason that the protonated canavanine exchanges all of its labile hydrogens is likely due to the same reason; its basicity and PA are lower than those

of arginine because of the oxygen substitution. However, PA differences are not the only factors that affect H/D exchange behavior.

In direct contrast to its monomeric form, the proton-bound arginine dimer exchanges all 15 of its labile hydrogen atoms at a faster rate than the proton-bound canavanine dimer, its less basic counterpart. This is surprising at first glance; however, the fact that the proton-bound arginine dimer can form a salt bridge complex may go a long way in explaining this discrepancy. Because one of the arginine molecules in the dimer exists as a zwitterion, proton transfer from a guanidine group on the side chain to the negatively charged carboxylate group can occur (refer to Figure 4.2). This would leave the guanidine group deprotonated so that it can accept a proton (deuteron) via the relay mechanism.<sup>8</sup> In this way, all of the dimer's labile hydrogen atoms could be exchanged. The fact that the exchanges of the canavanine dimer occur much more slowly than those of arginine lends support to this hypothesis. However, to confirm that such a mechanism is taking place, it would be necessary to calculate site-specific rate constants for both the canavanine and arginine proton-bound dimers.

#### 4.5 References

1. Price, W. D.; Jockusch, R. A.; Williams, E. R. *J. Am. Chem. Soc.* **1997**, *119*, 11988-11989.
2. Julian, R. R.; Hodyss, R.; Beauchamp, J. L. *J. Am. Chem. Soc.* **2001**, *123*, 3577-3583.
3. Jockusch, R. A.; Price, W. D.; Williams, E. R. *J. Phys. Chem. A* **1999**, *103*, 9266-9274.
4. Strittmatter, E. R.; Williams, E. R. *J. Phys. Chem. A* **2000**, *104*, 6069-6076.
5. Rosenthal, G. A. *Amino Acids* **2001**, *21*, 319-330.
6. Andriole, E. J.; Colyer, K. E.; Cornell, E.; Poutsma, J. C. *J. Phys. Chem. A* **2006**, *110*, 11501-11508.



7. Dookeran, N. N.; Harrison, A. G. *J. Mass Spectrom.* **1995**, *30*, 666-674.
8. Geller, O.; Lifshitz, C. *J. Phys. Chem. A* **2003**, *107*, 5654-5659.

## Chapter 5: Conclusions

### 5.1 Study of Protonated Lysine and its Homologs

Lysine, ornithine, DABA, and DAPA are diamino acids that differ only in the number of methylene groups in their side chains. Despite this structural similarity, lysine is a proteinogenic amino acid whereas ornithine, DABA, and DAPA are non-proteinogenic amino acids. In addition, these four compounds display different H/D exchange rates. Although protonated lysine, ornithine, DABA, and DAPA were observed to exchange all six of their labile hydrogens in an ESI mass spectrometer under H/D exchange conditions, DAPA had the largest rate coefficients and ornithine had, by far, the smallest rate coefficients for its exchanges. This is an unexpected trend when one considers the fact that ornithine has three methylene groups in its side chain. In other words, lysine, which has a longer side chain, and DABA, which has a shorter side chain, both displayed faster exchanges than ornithine.

To further investigate the reasons for this discrepancy in exchange rate coefficients, the structures of protonated lysine, ornithine, DABA, and DAPA were geometrically optimized at the B3LYP level of theory with the 6-31+G\*\* basis set using Gaussian 98W. The interaction of water (to substitute for the deuterating agent D<sub>2</sub>O) with protonated ornithine, DABA, and DAPA was also modeled at the same level of theory. By placing a water molecule near different sites of the amino acids and finding the transition states for the water to move from one site to another, it was possible to represent two different exchange mechanisms and to calculate the energetic barriers to these mechanisms. It was found that the barriers to exchange at the carboxylic acid of ornithine and DAPA via the flip-flop mechanism differed by only 0.8 kcal/mol; the

barriers to exchange at the amino groups of ornithine and DAPA via the relay mechanism differed by only 1.9 kcal/mol. Therefore, it is proposed that the barrier for the water to move from its position in the lowest energy structure to begin exchange at the amino groups is higher for ornithine than for lysine, DABA, and DAPA. Furthermore, this barrier to the initiation of exchange is responsible for the slow exchanges displayed by ornithine. To test this hypothesis, it will be necessary to find the global minima for the interaction of water with each of the four protonated amino acids and to calculate the aforementioned barriers.

### 5.2 Study of Protonated Arginine and Canavanine

The monomeric and dimeric forms of protonated arginine and its oxa-analog canavanine were studied under H/D exchange conditions in the same ESI mass spectrometer. The protonated arginine monomer did not undergo significant exchange, but the protonated canavanine monomer underwent exchange of all eight of its labile hydrogens. The proton-bound dimers of arginine and canavanine exchanged all 15 of their labile hydrogens. However, the rates of exchange were faster for the proton-bound arginine dimer than for the proton-bound canavanine dimer. A difference in proton affinity likely accounts for the difference in H/D exchange behavior of the monomers. The substitution of the  $\delta$ -methylene group in arginine for the oxygen atom in canavanine results in canavanine having a lower proton affinity. Thus, protonated canavanine is more likely than protonated arginine to undergo exchange with a weakly basic deuterating agent like D<sub>2</sub>O. In the case of the proton-bound dimers, it is proposed that arginine forms a salt-bridge complex in which one arginine is a zwitterion and the other is in a charge solvated form. This form would allow the exchange of all of the labile hydrogens in the

proton-bound arginine dimer via a relay mechanism. The slower exchanges of the proton-bound canavanine dimer appear to support this hypothesis in that canavanine is not expected to form a zwitterion in the gas phase because of its lower proton affinity. To confirm this hypothesis, however, it would be necessary to obtain site-specific rate constants for the dimers of arginine and canavanine instead of apparent rate constants. Thus, it would highly beneficial to review the data fitting procedures used throughout and either modify them or use a different fitting program altogether to obtain site-specific rate constants.